MitoFit Preprints 2023.6
https://doi.org/10.26124/mitofit:2023-0006

Experimental communication

Cite
Arias-Reyes C, Aliaga-Raduán F, Pinto-Aparicio R, Joseph V, Soliz J (2023) Mitochondrial plasticity in the retrosplenial cortex enhances ATP synthesis during acclimatization to hypoxia in mice but not in rats. MitoFit Preprints 2023.6. https://doi.org/10.26124/mitofit:2023-0006

Author contributions
C. A-R. performed or participated in all the experiments and data analyses; F. A-R and R. P-A. performed experiments and participated in analysis. C.A-R., V. J., and J. S. wrote the manuscript; C. A-R., V. J., and J. S. approved the manuscript.

Conflicts of interest
The authors declare that the research was conducted in the absence of any commercial or financial relationships that could be construed as a potential conflict of interest.

Online 2023-08-21

Data availability
Raw data used for this manuscript is available upon reasonable request to the corresponding authors.

Keywords
Acclimatization to hypoxia;
high altitude;
mitochondria;
brain;
metabolism

Mitochondrial plasticity in the retrosplenial cortex enhances ATP synthesis during acclimatization to hypoxia in mice but not in rats

Christian Arias-Reyes[1,2], Fernanda Aliaga-Raduán[1,2], Renata Pinto-Aparicio[1,3], Vincent Joseph[1*†], Jorge Soliz[1,2*†]

1 Centre de Recherche de l'Institute Universitaire de Cardiologie et de Pneumologie de Québec, Université Laval, Québec, QC, Canada.
2 Brain Research Institute, Bolivian Foundation of Altitude Sciences (BFAS). La Paz, Bolivia.
3 Department of Biochemistry, Université du Québec à Montréal, Montréal, QC, Canada.

* Corresponding authors:
Vincent Joseph: vincent.joseph@criucpq.ulaval.ca
Jorge Soliz: jorge.soliz@criucpq.ulaval.ca

†These authors have contributed equally to this work and share senior authorship.

Summary

Acclimatization to high altitude relies on adjustments of cellular metabolism that optimize oxygen use and energy production. In tissues with high energy demand and almost exclusive reliance on aerobic metabolism such as the brain, hypoxia is a particularly strong stressor, however, strategies to adjust metabolic pathways for successful high-altitude acclimatization remain poorly understood. Compared to SD rats, FVB mice show successful acclimatization to high altitude, we, therefore, used this model to investigate metabolic adjustments in the retrosplenial cortex (a key area of the brain involved in spatial learning and navigation) in normoxia and during acclimatization to hypoxia (12 % O_2 – 1, 7, and 21 days). We measured in simultaneous the rates of ATP synthesis and O_2 consumption in fresh permeabilized brain samples by coupled high-resolution respirometry and fluorometry. We quantified the

citrate synthase (CS) activity as an index of mitochondrial content, the transcriptional regulation of genes involved in mitochondrial dynamics; and the activity of enzymes representative of the glycolytic, aerobic, and anaerobic metabolism. Our findings show that acclimatization to hypoxia significantly increases ATP synthesis in mice and to a lower extent in rats. In mice, this occurs in parallel with a reduction of O_2 consumption, and a three-fold increase in the P»/O ratio. In rats, a six-fold increase in CS activity and altered mitochondrial dynamics gene expression are evident. Finally, activities of glycolytic, aerobic, or anaerobic enzymes remain overall unchanged in both species except for a transient glycolytic and anaerobic peak at day 7 in mice. Altogether, our results show that chronic hypoxia optimizes the efficiency of mitochondrial ATP synthesis in the retrosplenial cortex of mice. Contrastingly, rats sustain the production of ATP only by increasing mitochondrial content and altering mitochondrial dynamics, suggesting drastic mitochondrial malfunctions.

1. Introduction

Life at high altitudes requires adequate adjustments in oxygen utilization at systemic, cellular, and subcellular levels. The efficiency of these responses differs between species and underlie the survival and adaptation capacity at a given altitude. We recently described that Sprague-Dawley rats and FVB mice are a reliable model of divergent adaptation to hypoxia based on the fact that, when raised at high altitude (3,600 m – La Paz, Bolivia) for several generations rats show excessive erythrocytosis, signs of pulmonary hypertension, and reduced whole-body metabolism, which are signs of impaired adaptation, on the contrary, mice display low hematocrit, reduced arterial pulmonary pressure, and maintain an elevated metabolic rate, in accordance with traits observed in other species successfully adapted to high-altitude (Jochmans-Lemoine, Villalpando, Gonzales, Valverde, Soria, & Joseph, 2015). We have proposed that these physiological limitations have prevented rats to colonize high-altitude habitats, while mice, being pre-adapted to high altitude due to their phylogeographical origin the mid and highlands close to the Himalayan region (Bonhomme & Searle, 2012), have successfully established viable colonies at up to 5,000 m of altitude in South America (Christian Arias-Reyes, Soliz, & Joseph, 2021; Jochmans-Lemoine, Shahare, Soliz, & Joseph, 2016; Jochmans-Lemoine et al., 2015). Since this divergent response to hypoxia can be conveniently replicated in laboratory conditions, it allows the study of how reversible organ-specific responses arise during the first weeks of hypoxic exposure, namely acclimatization.

The brain is one of the most metabolically demanding organs in mammals as it consumes around 15 - 18 % of the whole-body energy expenditure (Wang, Zhang, Ying, & Heymsfield, 2012). Considering the high dependence of this organ on oxygen supply, how the brain deals with long-term hypoxia remains a mesmerizing question. Metabolic

depression and reduction of aerobic ATP production are among the responses to acute hypoxia that appear to be well preserved across a large range of hypoxia-tolerant species (Ramirez, Folkow, & Blix, 2007; Storz, Scott, & Cheviron, 2010), but the advantages of these responses during long-term exposure remain disputable as they might imply lethargy and functional impairments (Koester-Hegmann et al., 2019; Yan, Zhang, Shi, Gong, & Weng, 2010). Moreover, changes in anaerobic metabolic pathways might help support a reduction of mitochondrial ATP production (Erecińska & Silver, 2001; Ramirez, Folkow, & Blix, 2007), albeit temporarily. Nonetheless, to our knowledge, the rate and efficiency of mitochondrial ATP synthesis during acclimatization to hypoxia have never been directly measured.

Accordingly, we tested the hypothesis that the rate and efficiency of ATP synthesis are regulated during acclimatization to hypoxia. We used SD rats and FVB mice living at sea level and acclimatized to normobaric hypoxia for up to 3 weeks. We measured mitochondrial ATP synthesis, oxygen consumption rates, the concentration of mitochondrial and cytosolic proteins, the relative mRNA expression of genes involved in mitochondrial dynamics (i.e., fission, fusion, mitogenesis), and the activity of selected enzymes involved in aerobic and anaerobic metabolic pathways. We focused our studies on the retrosplenial cortex (RSC), an area of the brain particularly sensitive to hypoxia that is associated with a range of spatial and cognitive functions, including episodic memory, navigation, and self-referencing (Kleszka et al., 2020; Vann, Aggleton, & Maguire, 2009), and, thus, shall directly affect the ability of individuals to colonize high-altitude environments. We show that mice display significant reconfigurations at cellular and mitochondrial levels that optimize aerobic ATP production. In rats, this response is apparently restricted to energetically expensive increases in mitochondrial biogenesis.

2. Methods

2.1. Animals

We used a total of 65 male adult (seven weeks old) Sprague-Dawley rats (Charles River) and 62 FVB-NJ mice (Jackson). All the animals were housed at the animal care facilities of the “Centre de Recherche de l’Institut Universitaire de Cardiologie et de Pneumologie de Québec” (CR-IUCPQ) with food and water *ad libitum* and exposed to 12 h:12 h light:dark cycles. All experimental procedures were in concordance with the Canadian Council of Animal Care and approved by the Animal Protection Committee of Laval University, Québec, Canada.

2.2. Exposure to Hypoxia

All experimental procedures were in concordance with the Canadian Council of Animal Care and approved by the Animal Protection Committee of Laval University, Québec, Canada.

2.3. Tissue Sampling

After hypoxic exposure, animals were anesthetized and euthanized. Immediately after the sacrifice, the brain was dissected and the retrosplenial area of the cortex was extracted.

For mitochondrial function assays, approximately 2 mg of the sample were promptly weighed after removing liquid excess by gently taping around the sample with drying paper until no drops were visible, and transferred into ice-cold respirometry medium MiR05 (0.5 mM EGTA, 3 mM $MgCl_2*6H_2O$, 60 mM K-lactobionate, 20 mM taurine, 10 mM KH_2P0_4, 20 mM HEPES, 110 mM sucrose, and 1 g/L bovine serum albumin pH= 7) supplemented with saponin (50 µg/ml) for permeabilization of the cell membranes as previously described (C. Arias-Reyes, Losantos-Ramos, Gonzales, Furrer, & Soliz, 2019; Christian Arias-Reyes, Soliz, & Joseph, 2021). The samples used for ATP production rate measurements were kept in $MgCl_2$-free MiR05 supplemented with saponin. The remaining portions of the tissue were frozen on dry ice and stored at -80 °C for later use.

2.4. Mitochondrial ATP production and O_2 consumption rates

Brain samples were transferred inside the respirometry chambers of the Oxygraph-2k (Oroboros Instruments – Innsbruck, Austria) filled with the corresponding MiR05 medium supplemented with saponin, and left incubating for 15 minutes. Mitochondrial respiration data were recorded using the software DatLab v.7.4.0.4 (Oroboros Instruments – Innsbruck, Austria). The mass-specific rates of oxygen consumption (OCR - pmol $O_2 \cdot s^{-1} \cdot mg^{-1}$) or ATP production (pmol $ATP \cdot s^{-1} \cdot mg^{-1}$), were quantified using three specific protocols intended to respectively measure: 1) The ATP production rate and the ratio of ATP produced per atom of oxygen used (P»/O), 2) O_2 consumption in LEAK and OXPHOS states, and 3) the maximum O_2 consumption in the uncoupled ET state. For each protocol different groups of animals were used, the number of rats and mice in each group is reported in the tables and figures. The LEAK state results from the slippage of protons across the inner mitochondrial membrane toward the mitochondrial matrix in presence of mitochondrial substrates but in the absence of ADP. The OXPHOS state accounts for the respiration of mitochondria when the electron flux and oxygen consumption (oxidation) are coupled with ATP synthesis (phosphorylation). The ET state occurs when the electron flux and oxygen consumption are uncoupled from the ATP synthesis by the addition of a protonophore in presence of mitochondrial substrates and ADP (Gnaiger et al., 2020).

ATP Production Rate and P»/O ratio: For these assays, a $MgCl_2$-free MiR05 medium supplemented with saponin was used, as previously described by Salin et al. (2016) and Chinopoulos, Kiss, Kawamata, and Starkov (2014). This assay determines the ATP concentration by measuring the fluorescence produced by Magnesium Green™ (MgGreen) when it binds to the free Mg^{+2} molecules released during ADP-ATP exchange across the mitochondrial membrane. Briefly, using the Fluo-2K module in the Oxygraph-2K (excitation: 465 nm; detection: 525 nm), first, we determined the binding affinity of magnesium for ADP ($K_{d\text{-}ADP}$) and ATP ($K_{d\text{-}ATP}$) in $MgCl_2$-free MiR05 medium supplemented with saponin (50 µg/L). In absence of any sample, 2.1 µM MgGreen, 0.1 mM EGTA, 15 µM EDTA, 5 mM pyruvate, 0.5 mM malate, 10 mM glutamate, and 50 mM succinate were injected separately into the chamber of the Oxygraph-2k. Immediately after, 10 stepwise additions of 0.1 mM $MgCl_2$ were made. Finally, in two separate assays, 25 injections of ADP (0.25 mM per injection) or ATP (0.2 mM per injection) were added. $K_{d\text{-}ADP}$ and $K_{d\text{-}ATP}$ were estimated with the least squares fitting method described by Chinopoulos et al. (2014). We calculated $K_{d\text{-}ADP}$ = 1.722 mM and $K_{d\text{-}ATP}$ = 0.369 mM.

Then, for each sample, the OCR and MgGreen fluorescence were measured simultaneously. After 15 minutes of incubation, 2.1 µM MgGreen, 0.1 mM EGTA, 15 µM EDTA, 5 mM pyruvate, 0.5 mM malate, 10 mM glutamate, and 50 mM succinate were

injected into the analysis chambers containing the samples, followed by 10 stepwise additions of 0.1 mM $MgCl_2$ to calibrate the fluorescence signal. The ATP synthesis was triggered by adding 2 mM ADP, at this point, the measured OCR and MgGreen fluorescence are representative of raw oxygen ($J_{O_2\ raw}$) and ATP ($J_{ATP_{raw}}$) fluxes respectively. After approximately 15 minutes, 4 µM carboxylatractyloside (cATR) was injected to stop the ADP-ATP exchange across the mitochondrial membrane, henceforth, the slope of the MgGreen fluorescence corresponds to the rate of ATP consumption by the action of ATPases ($J_{ATP_{LEAK}}$). Lastly, the mitochondrial respiration was inhibited with 0.5 µM rotenone and 2.5 µm antimycin A.

From the fluorescence of MgGreen, the concentration of free Mg^{+2} and then that of ATP was calculated as described by Chinopoulos et al. (2014). The rates $J_{ATP_{raw}}$ and $J_{ATP_{LEAK}}$ were estimated by linear regressions of the ATP concentration as a function of time. Since $J_{ATP_{raw}}$ represents the balance between the rates of ATP production and consumption ($J_{ATP_{LEAK}}$), the ATP production rate was calculated as $J_{ATP_{raw}}$ - $J_{ATP_{LEAK}}$. P»/O ratios were calculated as ATP production rate/(2*OCR).

Oxygen consumption rates under LEAK and OXPHOS states: After 15 minutes of incubation, 5 mM pyruvate and 2 mM malate were consecutively added to the assay chambers, followed by 10 mM glutamate, to activate the N pathway in the LEAK state. Then, timely injections of 2.5 mM ADP, 10 µM cytochrome *c* (to control the integrity of the outer mitochondrial membrane), 50 mM succinate, and 0.5 µM rotenone were made to record the OCR for N, N&S, and S pathways in OXPHOS state correspondingly (Doerrier, Garcia-Souza, Krumschnabel, Wohlfarter, Mészáros, & Gnaiger, 2018). Finally, 2.5 µM antimycin A (inhibitor of Complex III) was added to stop the mitochondrial respiration and the corresponding OCR was subtracted from all the other values to correct for non-mitochondrial respiration (ROX).

Maximum O_2 consumption in the uncoupled ET state: After 15 minutes of incubation, 5 mM pyruvate and 2 mM malate were injected into the recording chambers. Next, 2.5 mM ADP, 10 µM cytochrome *c*, and 20 µM CCCP (protonophore) were added to initiate the uncoupled mitochondrial respiration. Then, timely injections of 10 mM glutamate, 50 mM succinate, and 0.5 µM rotenone were made to record the OCR for N, N&S, and S pathways during ET state correspondingly (Doerrier et al., 2018). ROX state was reached by the addition of 2.5 µm antimycin A and used for non-mitochondrial OCR correction. The maximum capacity of the electron transfer system (ETS maximum capacity) is defined as the mitochondrial OCR when all the electron-transfer pathways relevant to the analyzed tissue are active during the ET state, which in our experiments corresponds to the N&S pathway. The flux control ratio (FCR) was calculated for each sample as the OCR for each electron-transfer pathway, N and S, divided by the OCR for N&S. FCR values have the advantage of internal normalization of mitochondrial content (Gnaiger et al., 2020) and represent the fraction of the ETS maximum capacity supported by N or S pathways.

Activity of cytochrome *c* oxidase (CIV): The reduction of O_2 into H_2O catalyzed by CIV was quantified by measuring the OCR as described previously (Christian Arias-Reyes, Soliz, & Joseph, 2021). Briefly, at the end of the ET respiration experiments 2 mM ascorbate and 0.5 mM N,N,N′,N′-Tetramethyl-p-phenylenediamine dihydrochloride (TMPD) were injected into the Oxygraph-2K chambers to activate CIV. Chemical

autoxidation of TMPD was corrected by measuring the OCR after the addition of 100 mM sodium azide.

2.5. Proteins quantification and enzymatic assays

Protein concentration: Samples (50 – 100 mg) were homogenized in PBS-EDTA buffer (0.5 mM) and the mitochondrial and cytosolic fractions were obtained as described previously (Jochmans-Lemoine et al., 2018). Aliquots of both fractions were stored at -80 °C until analysis. The protein concentration was determined in both fractions using the BCA Protein Assay Kit (Bio Basic, SK3021).

Activity of hexokinase, lactate dehydrogenase, and pyruvate dehydrogenase: We used the cytosolic fraction to measure the activity of hexokinase (HK) and lactate dehydrogenase (LDH) via colorimetric assays (respectively ab136957, ab102526, Abcam), and the mitochondrial fraction to measure the activity of pyruvate dehydrogenase (PDH) using the PDH Enzyme Activity Microplate Assay Kit (ab109902; Abcam).

Citrate synthase (CS): CS catalyzes the reaction between acetyl CoA and oxaloacetic acid (OAA) to form citrate and CoA-SH inside mitochondria. CoA-SH reacts with 5,5′-dithiobis(2-nitrobenzoic acid) (DTNB) producing the colored product 5-thio-2-nitrobenzoic acid (TNB) that can be quantified by spectrophotometry at 412 nm. We measured the CS activity in the mitochondrial fraction by monitoring for 3 minutes the formation of TNB on an assay mix containing 0.1 mM acetyl CoA, 0.4 mM OAA, and 0.1 mM DTNB in 100 mM TRIS buffer (pH=8). A solution of 1 U/ml CS (Sigma Aldrich, C3260) was used as the positive control.

2.6. mRNA expression

Approximately 40 mg of brain cortex tissue per sample were used to extract RNA with the RNeasy Lipid Tissue Mini kit (74804; QIAGEN). Purity was tested by spectroscopy in the Nanodrop 2000 (ThermoScientific) system and RNA integrity was assessed by denaturing RNA electrophoresis. Immediately after extraction, cDNA was synthesized using 1 µg of RNA using the iScript™ cDNA Synthesis Kit (1708891) kit. cDNA samples were diluted 1/200 and 5 µl were amplified in a Corbett Rotor-Gene RG6000 thermal cycler with SsoAdvanced Universal SYBR® Green Supermix (1725272; BIORAD) by quantitative real-time PCR (qRT-PCR). The sequences of the primers we used are in Table S1. The relative mRNA expression for each evaluated gene was quantified with the ΔΔCt method (Riedel, Düker, Fekete-Drimusz, Manns, Vondran, & Bock, 2014) using the ribosomal protein lateral stalk subunit P0 (RPLPO) and hypoxanthine phosphoribosyltransferase 1 (HPRT1) as reference genes.

2.7. Transmission electron microscopy

Blocks of approximately 1 mm^3 were cut from the retrosplenial cortex of fresh brain samples taken from two individuals per selected exposure group (normoxia, 7 days hypoxia, and 21 days hypoxia). The sample blocks were immediately saved in fixation solution (2.5 % glutaraldehyde and 1.6 % formaldehyde in cacodylate buffer) and then stored overnight at 4 °C. Sample blocks were sent to the Institute of Integrative Biology and Systems (IBIS) from Laval University to be processed (prepared, stained, and cut in

slides) by specialized personnel. Briefly, fixated sample blocks were post fixated in a solution of 1 % osmium tetroxide (OsO_4) in cacodylate buffer (pH=7.2) for 90 minutes at room temperature and then dehydrated in ethanol series (30 %, 50 %, 70 %, 95 %, 100 % - 10 minutes each). In following, series of infiltration procedures were performed in the following order: solution of propylene oxide and EPON812® (1:1 – overnight at room temperature), EPON812® without DMP30 (2,4,6-Tris-(dimethylaminomethyl)phenol - overnight at room temperature), and EPON812® with DMP30 (2 h at room temperature). Finally, infiltrated samples were placed in molds with fresh DMP30-containing EPON812® solution and let solidify for 3 days at 60 °C. Once solidified, the sample blocks were cut into 80 nm sections on a Reichert Jung Ultracut E microtome and stained with 2 % uranyl acetate ($C_4H_6O_6U$ - 8 minutes) and 3 % lead citrate ($C_{12}H_{10}O_{14}Pb_3$ – 5 minutes). Sections were observed with a JEOL TEM-1230 (Tokyo, Japan) microscope using 80 kV high tension. All reagents were bought from Electron Microscopy Sciences (Hatfield - Pennsylvania, USA). The mitochondrial abundance was quantified in 50 randomly selected images. The mitochondrial area (summation the area of all mitochondria visible on a field of view), length, width, circularity, cristae abundance, and total cristae area (summation the area of all cristae visible on a field of view) were quantified using Image J software (National Institutes of Health, USA) in 300 randomly selected mitochondria per exposure group. The cristae volume density index was calculated as total cristae area/ total mitochondrial area on a field of view.

2.8. Data and statistical analysis

Data of ATP production rate, P»/O ratio, LEAK state respiration, ET state respiration, mitochondrial and cytosolic protein concentration, mRNA expression (DRP1, DNM2, MFN1, MFN2, TFAM, NRF1, and PGC1-α), and all the enzymatic activity assays (CIV, CS, HK, PDH, and LDH), were analyzed by standard two-way ANOVA tests, where species (rats and mice), and exposure (normoxia; 1 day, 7 days, and 21 days of hypoxia) were the independent factors. OXPHOS respiration data were analyzed by a two-way mixed-design ANOVA test, where OCR was the dependent variable, species (rats and mice), and exposure (normoxia; 1 day, 7 days, and 21 days of hypoxia) were the between-subjects factors, and the electron-transfer pathways (N, S, N&S) were the repeated measures. The effect of acclimatization to hypoxia (normoxia; 1 day, 7 days, and 21 days of hypoxia) over the mitochondrial abundance, ultrastructure (surface area, length, width, circularity, cristae abundance, cristae area, and cristae volume density) was analyzed using one-way ANOVA tests for each measured parameter.

For all the analyses, when significant differences in factors or interaction were found, post-hoc Fisher's Least Significance Difference multiple comparison tests were performed. The statistical significance was set to $p<0.05$. Data are presented as means ± SD unless stated differently.

3. Results

The probabilities calculated for all pairwise comparisons mentioned below are shown in Table 1.

3.1. Acclimatization to hypoxia induces more efficient ATP production in the retrosplenial cortex, transiently in rats, but sustainedly in mice.

We measured the ATP production rate during OXPHOS respiration by activating the N&S pathway as shown in Figure 1A. Under normoxic conditions, rats and mice synthesize ATP at roughly similar rates, however, hypoxia significantly affects both species, although, producing different response patterns (Two-way ANOVA $F_{species}$ = 44; d.f.= 1, 30; p<0.001; $F_{exposure}$ = 15.5; d.f.= 3, 30; p<0.001; $F_{species\_X\_exposure}$ = 2.49; d.f.= 3, 30; p=0.08 - Table 2). In rats, a strong (+130 %) but transient, rise in the rate of ATP production occurred at hypoxic day 7 but was restored to normoxic levels by day 21. Contrastingly, in mice, the ATP production rate increased gradually from day one of hypoxic exposure until reaching a plateau by day 7. At the plateau stage, the production of ATP was 2.5 times faster than in the corresponding normoxic controls (Fig. 1B).

Next, we calculated the P»/O ratio as a classical indicator of the efficiency of the aerobic synthesis of ATP. In normoxic animals, we obtained values of 1.74 ± 0.16 and 2.58 ± 1.13 for rats and mice respectively (Table 2). Hypoxic exposure produced a significant elevation of P»/O ratios in both species (Two-way ANOVA $F_{species}$ = 18; d.f.= 1, 30; p<0.001; $F_{exposure}$ = 8.18; d.f.= 3, 30; p=0.0004; $F_{species\_X\_exposure}$ = 1.63; d.f.= 3, 30; p=0.203). In rats, P»/O peaked at 4.54 ± 1.19 after 7 days of hypoxia and returned to normoxic control levels by day 21. Noticeably, in mice, P»/O reached a plateau of elevated values after one day of hypoxia (at day 7 P»/O = 6.08 ± 1.68) and remained stable until day 21 inclusively (Fig. 1C).

3.2. Mitochondrial respiration is transiently upregulated in rats but reduced in mice during acclimatization to hypoxia.

A representative recording of mitochondrial oxygen consumption rates (OCR) during the OXPHOS state is displayed in Figure 2A. We found that acclimatization to hypoxia for 21 days affects mitochondrial respiration differently in the retrosplenial cortex of rats and mice (Two-way mixed design ANOVA $F_{species}$= 101.31; d.f.= 1, 34; p<0.0001; $F_{exposure}$= 5.98; d.f.= 3, 34; p=0.002; $F_{species\_X\_exposure}$= 4.57; d.f.= 3, 34; p=0.009). In general, rats have significantly lower OCR values than mice both in normoxia and throughout hypoxic acclimatization, however, once exposed to hypoxia, different acclimatization patterns occur in both species. In rats, the N&S respiration transiently increases (+66 %) between hypoxic days 1 and 7, and then, it is restored to normoxic control levels by day 21. Contrastingly, in mice, it drops by 14 % on hypoxic day 1. While this is temporarily restored after 7 days, a further reduction (-28 %) takes place by day 21 (Fig. 2B). These changes involve exclusively the S pathway in rats, whereas, in mice, both pathways, N (Fig. 2C) and S (Fig. 2D), take part. OCR values are detailed in Table 3. Furthermore, LEAK respiration was unaffected by hypoxic acclimatization in rats. Mice, on the other hand, showed a 40 % decline in LEAK after hypoxic day 21 (Two-way ANOVA $F_{species}$ = 60.7; d.f.= 1, 34; p<0.001; $F_{exposure}$ = 5.16; d.f.= 3, 34; p=0.005; $F_{species\_X\_exposure}$ = 4.38; d.f.= 3, 34; p=0.01 - Fig. 2E). It is noteworthy that a lower LEAK represents an improved efficiency of the ETS for ATP production.

Table 1. Probabilities (*p*) for Fisher's LSD pairwise comparisons.

	Rats				Mice				Rats vs mice
	Nx	1 day Hx	7 days Hx	21 days Hx	Nx	1 day Hx	7 days Hx	21 days Hx	vs same exposure
ATP production									
Nx	-	0.579	<0.001	0.176	-	0.015	<0.001	<0.001	0.225
1 day Hx	0.579	-	<0.001	0.054	0.015	-	0.03	0.146	<0.001
7 days Hx	<0.001	<0.001	-	0.026	<0.001	0.03	-	0.296	0.004
21 days Hx	0.176	0.054	0.026	-	<0.001	0.146	0.296	-	<0.001
P»/O ratio									
Nx	-	0.703	0.003	0.103	-	0.019	0.002	0.007	0.355
1 day Hx	0.703	-	<0.001	0.04	0.019	-	0.41	0.991	<0.001
7 days Hx	0.003	<0.001	-	0.136	0.002	0.41	-	0.363	0.13
21 days Hx	<0.001	0.04	0.136	-	0.007	0.991	0.363	-	0.04
OXPHOS - OCR									
NS pathway									
Nx	-	<0.001	<0.001	0.299	-	0.03	0.873	<0.001	<0.001
1 day Hx	<0.001	-	0.981	0.005	0.03	-	0.02	0.034	<0.001
7 days Hx	<0.001	0.981	-	0.003	0.873	0.02	-	<0.001	<0.001
21 days Hx	0.299	0.005	0.003	-	<0.001	0.034	<0.001	-	<0.001
N pathway									
Nx	-	0.113	0.164	0.624	-	0.192	0.476	0.001	<0.001
1 day Hx	0.113	-	0.788	0.241	0.192	-	0.551	0.047	<0.001
7 days Hx	0.164	0.788	-	0.342	0.476	0.551	-	0.01	<0.001
21 days Hx	0.624	0.241	0.342	-	0.001	0.047	0.01	-	0.007
S pathway									
Nx	-	0.025	0.007	0.614	-	0.08	0.958	0.019	<0.001
1 day Hx	0.025	-	0.692	0.064	0.08	-	0.071	0.545	0.076
7 days Hx	0.007	0.692	-	0.019	0.958	0.071	-	0.017	0.001
21 days Hx	0.614	0.064	0.019	-	0.019	0.545	0.017	-	0.002
LEAK									
Nx	-	0.315	0.065	0.364	-	0.661	0.735	<0.001	<0.001
1 day Hx	0.315	-	0.405	0.886	0.661	-	0.439	0.001	<0.001
7 days Hx	0.065	0.405	-	0.308	0.735	0.439	-	<0.001	<0.001
21 days Hx	0.405	0.886	0.308	-	<0.001	0.001	<0.001	-	0.328
RCR									
Nx	-	0.139	0.182	0.903	-	0.591	0.871	0.122	0.649
1 day Hx	0.139	-	0.825	0.097	0.591	-	0.708	0.041	0.119
7 days Hx	0.182	0.825	-	0.129	0.871	0.708	-	0.089	0.3
21 days Hx	0.825	0.097	0.129	-	0.122	0.041	0.089	-	0.03

	Rats				Mice				Rats vs mice
	Nx	1 day Hx	7 days Hx	21 days Hx	Nx	1 day Hx	7 days Hx	21 days Hx	vs same exposure
ETS Max. capacity									
Nx	-	0.058	0.023	0.761	-	0.047	0.994	0.393	0.508
1 day Hx	0.058	-	0.476	0.163	0.047	-	0.069	0.205	0.003
7 days Hx	0.023	0.476	-	0.066	0.994	0.069	-	0.449	0.11
21 days Hx	0.476	0.163	0.066	-	0.393	0.205	0.449	-	0.633
FCR									
N pathway									
Nx	-	>0.999	0.683	0.443	-	0.618	0.771	0.227	0.221
1 day Hx	>0.999	-	0.683	0.443	0.618	-	0.789	0.086	0.453
7 days Hx	0.683	0.683	-	0.168	0.771	0.789	-	0.097	0.394
21 days Hx	0.443	0.443	0.168	-	0.227	0.086	0.097	-	<0.001
S pathway									
Nx	-	>0.999	0.683	0.443	-	0.237	0.556	<0.001	0.624
1 day Hx	>0.999	-	0.683	0.443	0.237	-	0.462	0.027	0.118
7 days Hx	0.683	0.683	-	0.168	0.556	0.462	-	0.001	0.406
21 days Hx	0.443	0.443	0.168	-	<0.001	0.027	0.001	-	0.013
CIV activity									
Nx	-	0.913	0.352	0.025	-	0.114	0.693	0.805	0.138
1 day Hx	0.913	-	0.248	0.014	0.114	-	0.332	0.199	0.777
7 days Hx	0.352	0.248	-	0.002	0.693	0.332	-	0.864	0.962
21 days Hx	0.248	0.014	0.002	-	0.805	0.199	0.864	-	<0.001
Mitochondrial content and protein concentration									
CS activity									
Nx	-	0.7	0.769	0.01	-	0.505	<0.001	0.122	<0.001
1 day Hx	0.7	-	0.927	0.025	0.505	-	0.003	0.357	<0.001
7 days Hx	0.769	0.927	-	0.02	<0.001	0.003	-	0.022	0.093
21 days Hx	0.927	0.025	0.02	-	0.122	0.357	0.022	-	0.068
Mitochondrial proteins									
Nx	-	0.8977	0.3098	<0.0001	-	<0.0001	<0.0001	<0.0001	<0.0001
1 day Hx	0.8977	-	0.3727	<0.0001	<0.0001	-	<0.0001	<0.0001	<0.0001
7 days Hx	0.3098	0.3727	-	<0.0001	<0.0001	<0.0001	-	0.0006	<0.0001
21 days Hx	0.3727	<0.0001	<0.0001	-	<0.0001	<0.0001	0.0006	-	<0.0001
Cytosolic proteins									
Nx	-	0.046	0.001	<0.0001	-	<0.0001	<0.0001	<0.0001	0.075
1 day Hx	0.046	-	0.168	<0.0001	<0.0001	-	<0.0001	<0.0001	<0.0001
7 days Hx	0.001	0.168	-	0.004	<0.0001	<0.0001	-	0.239	<0.0001
21 days Hx	0.168	<0.0001	0.004	-	<0.0001	<0.0001	0.239	-	<0.0001

	Rats				Mice				Rats vs mice
	Nx	1 day Hx	7 days Hx	21 days Hx	Nx	1 day Hx	7 days Hx	21 days Hx	vs same exposure
Relative ATP production and oxygen consumption rates									
ATP/CS									
Nx	-	0.0006	0.752	<0.0001	-	0.0108	<0.0001	<0.0001	>0.9999
1 day Hx	0.0006	-	0.0001	0.3465	0.0108	-	<0.0001	<0.0001	<0.0001
7 days Hx	0.752	0.0001	-	<0.0001	<0.0001	<0.0001	-	<0.0001	<0.0001
21 days Hx	0.0001	0.3465	<0.0001	-	<0.0001	<0.0001	<0.0001	-	<0.0001
OCR/CS									
Nx	-	0.8518	0.588	<0.0001	-	0.7542	<0.0001	0.0001	>0.9999
1 day Hx	0.8518	-	0.7528	<0.0001	0.7542	-	<0.0001	0.0003	0.9135
7 days Hx	0.588	0.7528	-	<0.0001	<0.0001	<0.0001	-	<0.0001	<0.0001
21 days Hx	0.7528	<0.0001	<0.0001	-	0.0001	0.0003	<0.0001	-	0.015
Mitochondrial dynamics									
DRP1									
Nx	-	0.066	0.036	0.0459	-	0.3059	0.4302	0.4401	0.9027
1 day Hx	0.066	-	0.0004	0.0005	0.3059	-	0.8095	0.7962	0.0049
7 days Hx	0.036	0.0004	-	0.9087	0.4302	0.8095	-	0.9862	0.2075
21 days Hx	0.0004	0.0005	0.9087	-	0.4401	0.7962	0.9862	-	0.243
DNM2									
Nx	-	0.3227	0.0034	0.0014	-	0.1669	0.3131	0.2703	0.4169
1 day Hx	0.3227	-	0.0003	0.0001	0.1669	-	0.6951	0.9713	0.0035
7 days Hx	0.0034	0.0003	-	0.7078	0.3131	0.6951	-	0.7762	0.1705
21 days Hx	0.0003	0.0001	0.7078	-	0.2703	0.9713	0.7762	-	0.2509
MFN1									
Nx	-	0.0457	0.0624	0.0408	-	0.066	0.0027	0.0125	0.5137
1 day Hx	0.0457	-	0.0005	0.0003	0.066	-	0.1674	0.4468	0.6345
7 days Hx	0.0624	0.0005	-	0.8369	0.0027	0.1674	-	0.5216	<0.0001
21 days Hx	0.0005	0.0003	0.8369	-	0.0125	0.4468	0.5216	-	<0.0001
MFN2									
Nx	-	0.0464	0.0157	0.0182	-	0.0517	0.8214	0.9523	0.8639
1 day Hx	0.0464	-	<0.0001	0.0001	0.0517	-	0.0813	0.0457	0.1225
7 days Hx	0.0157	<0.0001	-	0.9486	0.8214	0.0813	-	0.7753	0.0314
21 days Hx	<0.0001	0.0001	0.9486	-	0.9523	0.0457	0.7753	-	0.0108
TFAM									
Nx	-	0.0464	0.0157	0.0182	-	0.915	0.289	0.3631	0.6951
1 day Hx	0.0464	-	<0.0001	0.0001	0.915	-	0.2449	0.311	0.0155
7 days Hx	0.0157	<0.0001	-	0.9486	0.289	0.2449	-	0.8764	0.0031
21 days Hx	<0.0001	0.0001	0.9486	-	0.3631	0.311	0.8764	-	0.0053

	Rats				Mice				Rats vs mice
	Nx	**1 day Hx**	**7 days Hx**	**21 days Hx**	**Nx**	**1 day Hx**	**7 days Hx**	**21 days Hx**	**vs same exposure**
NRF1									
Nx	-	0.0022	0.0028	0.0107	-	0.7082	0.4225	0.8209	0.7429
1 day Hx	0.0022	-	<0.0001	<0.0001	0.7082	-	0.6658	0.8821	0.0025
7 days Hx	0.0028	<0.0001	-	0.5794	0.4225	0.6658	-	0.5625	0.0008
21 days Hx	<0.0001	<0.0001	0.5794	-	0.8209	0.8821	0.5625	-	0.0136
PGC1-α									
Nx	-	0.0299	0.0922	0.0636	-	0.5381	0.7986	0.2918	0.7677
1 day Hx	0.0299	-	0.5841	0.719	0.5381	-	0.717	0.6546	0.1786
7 days Hx	0.0922	0.5841	-	0.8502	0.7986	0.717	-	0.4204	0.2428
21 days Hx	0.5841	0.719	0.8502	-	0.2918	0.6546	0.4204	-	0.575

Mitochondrial ultrastructure

Mitochondrial abundance

Nx	-	-	-	-	-	-	<0.0001	0.0568	-
1 day Hx	-	-	-	-	-	-	-	-	-
7 days Hx	-	-	-	-	<0.0001	-	-	<0.0001	-
21 days Hx	-	-	-	-	0.0568	-	<0.0001	-	-

Mitochondrial surface area

Nx	-	-	-	-	-	-	0.048	0.0114	-
1 day Hx	-	-	-	-	-	-	-	-	-
7 days Hx	-	-	-	-	0.048	-	-	0.5961	-
21 days Hx	-	-	-	-	0.0114	-	0.5961	-	-

Mitochondrial length

Nx	-	-	-	-	-	-	0.0014	0.0002	-
1 day Hx	-	-	-	-	-	-	-	-	-
7 days Hx	-	-	-	-	0.0014	-	-	0.645	-
21 days Hx	-	-	-	-	0.0002	-	0.645	-	-

Mitochondrial width

Nx	-	-	-	-	-	-	0.0165	0.0051	-
1 day Hx	-	-	-	-	-	-	-	-	-
7 days Hx	-	-	-	-	0.0165	-	-	0.72	-
21 days Hx	-	-	-	-	0.0051	-	0.72	-	-

Mitochondrial circularity

Nx	-	-	-	-	-	-	0.0522	0.0042	-
1 day Hx	-	-	-	-	-	-	-	-	-
7 days Hx	-	-	-	-	0.0522	-	-	0.3635	-
21 days Hx	-	-	-	-	0.0042	-	0.3635	-	-

	Rats				Mice				Rats vs mice
	Nx	1 day Hx	7 days Hx	21 days Hx	Nx	1 day Hx	7 days Hx	21 days Hx	vs same exposure
Cristae abundance									
Nx	-	-	-	-	-	-	0.0084	<0.0001	-
1 day Hx	-	-	-	-	-	-	-	-	-
7 days Hx	-	-	-	-	0.0084	-	-	0.1389	-
21 days Hx	-	-	-	-	<0.0001	-	0.1389	-	-
Cristae area									
Nx	-	-	-	-	-	-	0.0079	0.0027	-
1 day Hx	-	-	-	-	-	-	-	-	-
7 days Hx	-	-	-	-	0.0079	-	-	0.7642	-
21 days Hx	-	-	-	-	0.0027	-	0.7642	-	-
Cristae volume density									
Nx	-	-	-	-	-	-	0.3759	0.2108	-
1 day Hx	-	-	-	-	-	-	-	-	-
7 days Hx	-	-	-	-	0.3759	-	-	0.7218	-
21 days Hx	-	-	-	-	0.2108	-	0.7218	-	-
Enzymatic activity									
HK									
Nx	-	0.873	0.852	0.926	-	0.277	<0.001	0.595	<0.001
1 day Hx	0.873	-	0.978	0.801	0.277	-	<0.001	0.572	<0.001
7 days Hx	0.852	0.978	-	0.78	<0.001	<0.001	-	<0.001	<0.001
21 days Hx	0.978	0.801	0.78	-	0.595	0.572	<0.001	-	<0.001
LDH									
Nx	-	0.656	0.164	0.23	-	0.829	<0.001	0.936	<0.001
1 day Hx	0.656	-	0.08	0.48	0.829	-	<0.001	0.76	<0.001
7 days Hx	0.164	0.08	-	0.012	<0.001	<0.001	-	<0.001	<0.001
21 days Hx	0.08	0.48	0.012	-	0.936	0.76	<0.001	-	<0.001
PDH									
Nx	-	0.87	0.903	0.187	-	0.569	0.005	0.082	<0.001
1 day Hx	0.87	-	0.967	0.244	0.569	-	0.019	0.228	<0.001
7 days Hx	0.903	0.967	-	0.228	0.005	0.019	-	0.214	<0.001
21 days Hx	0.967	0.244	0.228	-	0.082	0.228	0.214	-	<0.001

Table 2. ATP production rates and P»/O ratios.

	Rats (mean ± S.D.)				Mice (mean ± S.D.)			
	Nx	1 day Hx	7 days Hx	21 days Hx	Nx	1 day Hx	7 days Hx	21 days Hx
ATP production rate (pmol ATP/s*mg)	286 ± 45.7	229.86 ± 39.8	670.21 ± 94.47	432.92 ± 325.16	417.3 ± 276.28	731.46 ± 102.85	1043.07 ± 45.86	913.3 ± 73.95
P»/O ratio	1.74 ± 0.16	1.42 ± 0.45	4.54 ± 1.19	3.24 ± 2.82	2.58 ± 1.13	5.13 ± 0.18	6.08 ± 1.68	5.14 ± 1.44

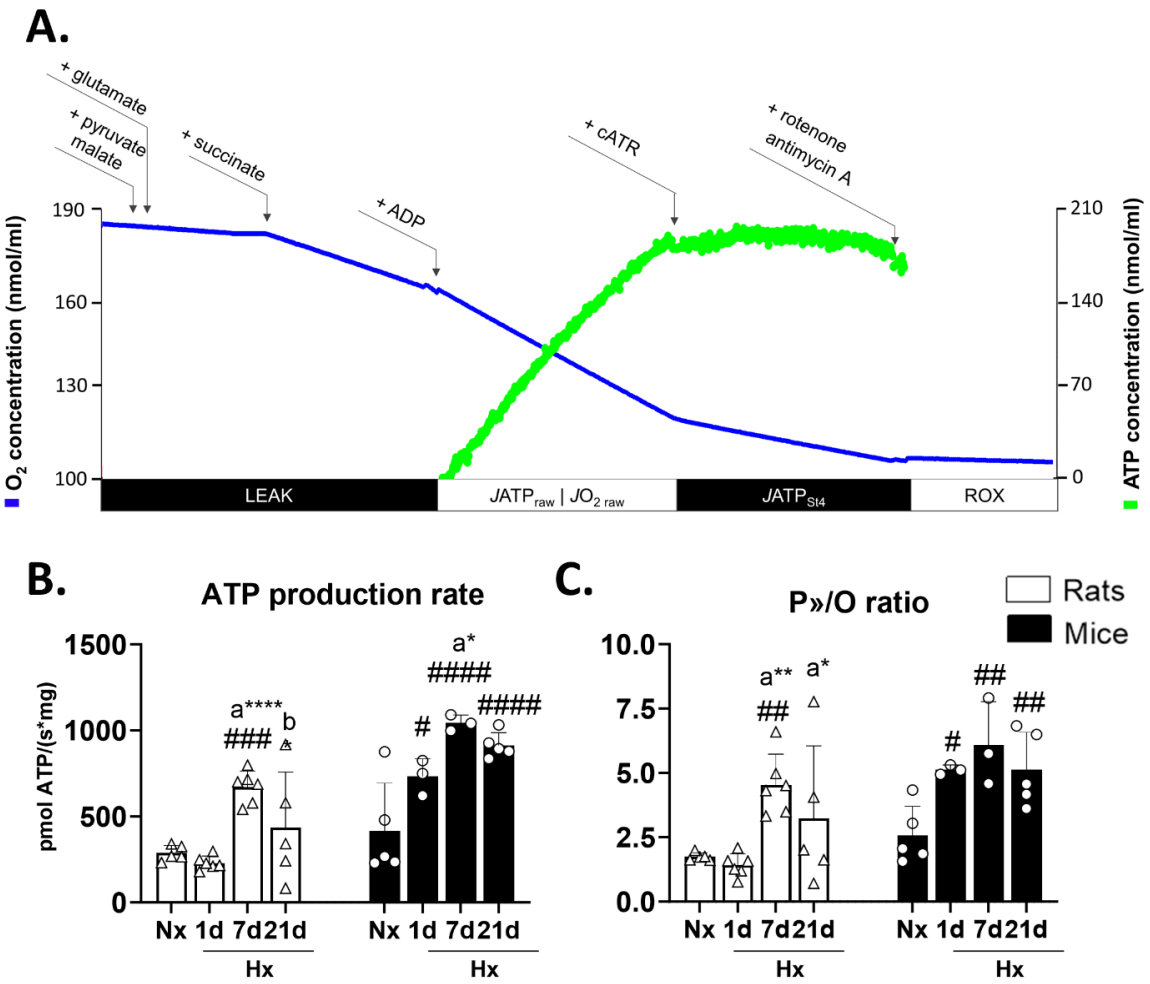

Figure 1. Mitochondrial ATP production rates in the retrosplenial cortex of rats and mice exposed to normoxia (Nx) or hypoxia (Hx) for 1, 7, or 21 days. The raw ATP production (JATP$_{raw}$), representing the balance between ATP production and consumption, was measured during active oxidative phosphorylation ($JO_{2\ raw}$) in the N&S electron-transfer pathway. Net ATP production rates were calculated as JATP$_{raw}$ - JATP$_{LEAK}$ (**A**). Hypoxic exposure triggered a temporary upsurge (+130 % - day 7) in the rate of ATP production in rats. In mice, such response was evidenced earlier (+ 73 % - day 1) and remained sustained until day 21 (+430 %; **B**). Such responses are linked with enhancements in the efficiency of ATP synthesis per atomic oxygen consumed (P»/O ratio) (**C**). $^{\#\#}p < 0.01$; $^{\#\#\#}p < 0.001$; and $^{\#\#\#\#}p < 0.0001$ vs. Nx; $^{a*}p < 0.05$; $^{a**}p < 0.01$; and $^{a****}p < 0.0001$ vs. Hx 1d; $^{b*}p < 0.05$ vs. Hx 7d. n = 3–6.

3.3. The ETS maximum capacity increases transiently in rats but not in mice during acclimation hypoxia.

In a third set of experiments, we evaluated the maximum capacity of the ETS by measuring the OCR during the ET state (Fig. 3A). Consistently with our OXPHOS$_{NS}$ respiration results, we found that acclimatization to hypoxia affects ETS maximum capacity differently in both species (Two-way ANOVA $F_{species}$ = 5.95; d.f.= 1, 33; p=0.02; $F_{exposure}$ = 1.6; d.f.= 3, 33; p=0.208; $F_{species\_X\_exposure}$= 2.96; d.f.= 3, 33; p=0.046). Rats showed a transitory increase (+40 %) in ETS maximum capacity between hypoxic days 1 to 7, which was restored to control levels by day 21. Mice, on the contrary, showed no

significant changes (Fig. 3B). These data were used to calculate the *FCR* (see methods) as the fraction of the ETS maximum capacity supported by the activity of either the N or S electron-transfer pathways. We found in both species, that regardless of hypoxic exposure, the N pathway participates significantly less (≈ 10 %) than the S pathway of the ETS maximum capacity (Two-way ANOVA $F_{state\_pathway}$ = 48.4; d.f.= 1, 99; p<0.001). Notwithstanding, the involvement of the N pathway remains unchanged along the process of acclimatization (Fig. 3C). Furthermore, after 21 days of exposure to hypoxia, the contribution of the S pathway to the ETS capacity was significantly reduced (-20 %) in mice while it remained unaffected in rats (Fig. 3D).

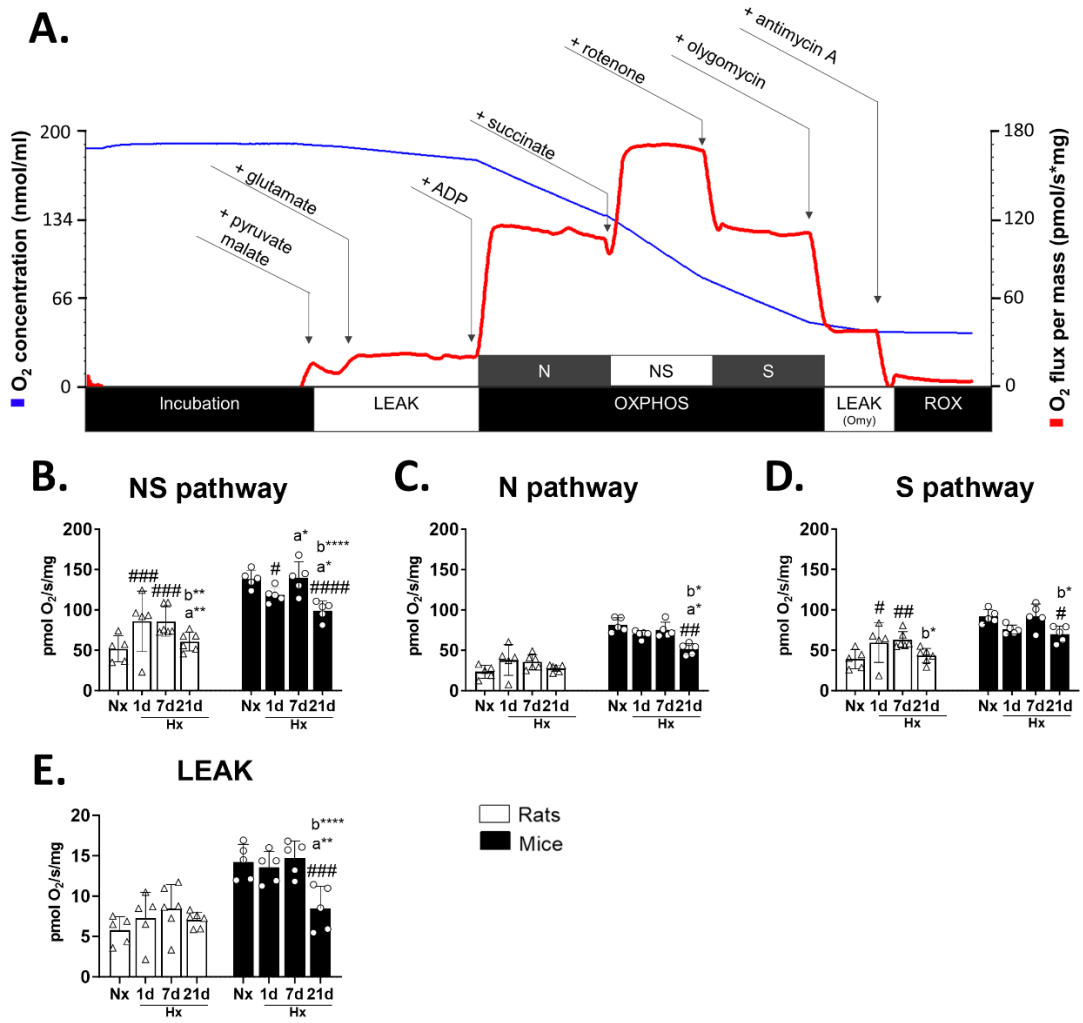

Figure 2. Mitochondrial oxygen consumption rates (OCR) during active oxidative phosphorylation (OXPHOS state) in the retrosplenial cortex of rats and mice exposed to normoxia (Nx) or hypoxia (Hx) for 1, 7, or 21 days (**A**). N&S respiration is transiently increased in rats after 1- and 7-day hypoxia; however, this effect disappears past 21 days. In mice, a depression of mitochondrial respiration (-14 %) is observed only after 21 days of hypoxia (**B**). The hypoxic mitochondrial response is independent of the N pathway in rats but involves both, N and S pathways in mice (**C**, **D**). LEAK respiration is unaffected in rats but drops by 40 % after 21-day hypoxia in mice (**E**). Seemingly higher Respiratory Control Ratios ($RCR=OCR_{N\&S}/OCR_{LEAK}$) at hypoxic day 21 occur only in mice (**F**). $^{\#}p < 0.05$; $^{\#\#}p < 0.01$; and $^{\#\#\#}p < 0.001$; $^{\#\#\#\#}p < 0.0001$ vs. Nx; $^{a*}p < 0.05$ and $^{a**}p < 0.01$ vs. Hx 1d; $^{b*}p < 0.05$; and $^{b****}p < 0.0001$ vs. Hx 7d. n = 5–6.

Table 3. Oxygen consumption rates (pmol O_2/s/mg) during OXPHOS state.

	Rats (mean ± S.D.)				Mice (mean ± S.D.)			
Pathway	**Nx**	**1 day Hx**	**7 days Hx**	**21 days Hx**	**Nx**	**1 day Hx**	**7 days Hx**	**21 days Hx**
NS	51.8 ± 16.2	85.9 ± 37.5	85.7 ± 18.2	60.8 ± 11.7	138.5 ± 10.8	118.6 ± 9.4	139.9 ± 19.8	99.2 ± 11.5
N	23.6 ± 8	38 ± 19	35.6 ± 9	27.8 ± 4.1	81.6 ± 8.8	69.8 ± 4.6	75.2 ± 9.6	51.6 ± 6.9
S	39 ± 12	59.5 ± 24.3	62.9 ± 10.1	43.4 ± 9.1	91.5 ± 8.5	75.6 ± 5.6	92 ± 15.1	70.1 ± 9.9
LEAK	14.2 ± 2.2	13.6 ± 1.9	14.7 ± 2.1	8.5 ± 2.8	5.8 ± 1.7	7.3 ± 3.2	8.5 ± 3	7.1 ± 1
RCR	9.9 ± 1.4	8.9 ± 1	9.6 ± 1.2	12.9 ± 5	9 ± 0.8	11.9 ± 2.5	11.5 ± 5.3	8.8 ± 2.3

In addition, we measured the activity of cytochrome *c* oxidase (CIV), the final step in the ETS, and the ultimate rate-limiting factor for electron flow (Table 4). We observed that acclimatization to hypoxia significantly reduced CIV activity after 21 days in rats but not in mice ($F_{species}$ = 7.9 d.f.= 1, 37; p=0.008; $F_{exposure}$ = 2.21; d.f.= 3, 37; p=0.104; Two-way ANOVA $F_{species\_X\_exposure}$ = 3.17; d.f.= 3, 37; p=0.035 - Fig. 3E).

3.4. Acclimatization to hypoxia increases mitochondrial content in the brain of rats, but not in mice.

All values for ATP production and OCR presented above are normalized to tissue mass and since mitochondrial mass may also be altered during acclimatization to hypoxia, we assessed the mitochondrial content by quantifying the activity of citrate synthase (CS - Table 5). We found that hypoxia affects both species, although in a dissimilar manner (Two-way ANOVA $F_{species}$ = 52.9 d.f.= 1, 39; p<0.001; $F_{exposure}$ = 4.16; d.f.= 3, 39; p=0.012; $F_{species\_X\_exposure}$ = 4.75; d.f.= 3, 39; p=0.006). Rats showed a marked augmentation in CS activity after 21 days (+500 %) of hypoxic exposure. In mice, on the other hand, CS activity remained stable during the first day of exposure. Then a transient 60 % drop in activity at day 7 was recovered by day 21 (Fig. 4A). Comparable patterns were observed for the concentration of mitochondrial proteins (Two-way ANOVA $F_{species}$ = 1255 d.f.= 1, 40; p<0.0001; $F_{exposure}$ = 73.3; d.f.= 3, 40; p<0.0001; $F_{species\_X\_exposure}$ = 78.2; d.f.= 3, 40; p<0.0001 - Fig. 4B), however, the relative increase in cytosolic proteins in rats was much less important (Two-way ANOVA $F_{species}$ = 500 d.f.= 1, 40; p<0.0001; $F_{exposure}$ = 8.96; d.f.= 3, 40; p=0.0001; $F_{species\_X\_exposure}$ = 53.4; d.f.= 3, 40; p<0.0001 - Fig. 4C).

Table 4. Cytochrome *c* oxidase activity.

	CIV activity (pmol O_2/s/mg)			
	Nx	**1 day Hx**	**7 days Hx**	**21 days Hx**
Rats (mean ± S.D.)	182 ± 45	179 ± 51	214 ± 61	110 ± 51
Mice (mean ± S.D.)	227 ± 34	186 ± 46	215 ± 39	221 ± 53

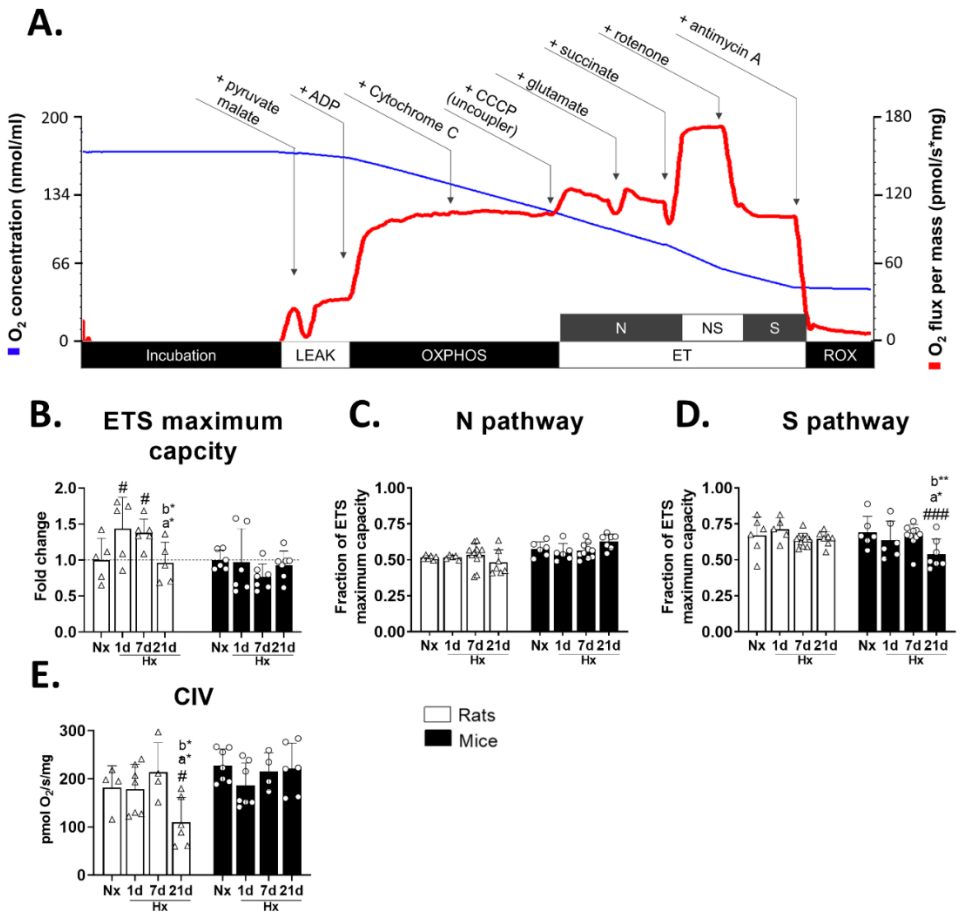

Figure 3. Activation of the mitochondrial N and S electron-transfer pathways as a fraction of the ETS maximum capacity in the retrosplenial cortex of rats and mice exposed to normoxia (Nx) or hypoxia (Hx) 1, 7, or 21 days. The OCR equivalent to the maximum ETS capacity was measured during the uncoupled ET state by activating the N&S electron transfer pathway (**A**). The ETS maximum capacity increases transiently during hypoxic acclimatization in rats, but control levels are restored by day 21. Contrastingly, ETS maximum capacity remains stable despite hypoxic exposure in mice (**B**). No effect of hypoxic acclimatization was observed in the involvement of N pathway in the ETS maximum capacity in any species (**C**). Contrastingly, the involvement of the S pathway is downregulated by 20 % after 21-day hypoxia only in mice (**D**). The activity of cytochrome *c* oxidase (CIV), the ultimate reducer of O_2 and thus the maximum work-rate controller in the ETS is reduced by 60 % after 21-day hypoxia in rats but not in mice (**E**). $^{\#}p < 0.05$ $^{\#\#\#}p < 0.001$ vs. Nx; $^{a*}p < 0.05$ vs. Hx 1d; $^{b*}p < 0.05$; $^{b**}p < 0.01$ vs. Hx 7d. n = 7–11.

Table 5. Citrate synthase activity, mitochondrial and cytosolic proteins concentration as a measurement of mitochondrial content.

	Rats (mean ± S.D.)				Mice (mean ± S.D.)			
	Nx	**1 day Hx**	**7 days Hx**	**21 days Hx**	**Nx**	**1 day Hx**	**7 days Hx**	**21 days Hx**
CS (IU/ mg tissue)	7.9E-4 ± 4E-4	1.6E-3 ± 4.4E-4	1.4E-3 ± 2.7E-4	6.4E-3 ± 2.7E-3	1.3E-2 ± 8.4E-3	1.2E-2 ± 3.7E-3	5.1E-3 ± 3.6E-3	1E-2 ± 2.9E-3
Mitochondrial proteins (µg prot./mg tissue)	2.3 ± 1.1	2.4 ± 1	2.9 ± 1	7.4 ± 1.1	202 ± 21	150 ± 13	60 ± 11	101 ± 21

Cytosolic proteins (µg prot./mg tissue)	116.2 ± 7.4	124 ± 8.2	129.2 ± 6.7	140.6 ± 6.6	109.3 ± 5.2	90 ± 6	68.8 ± 5.7	73.3 ± 5.2

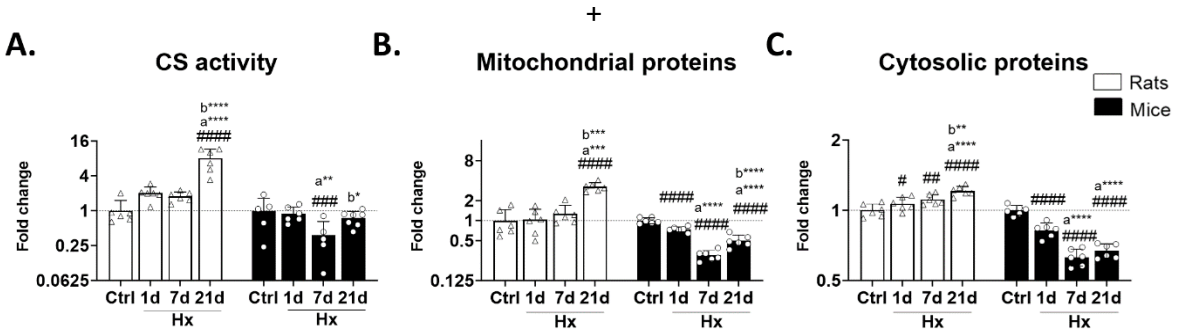

Figure 4. Citrate synthase (CS) activity and mitochondrial and cytosolic protein concentration in the retrosplenial cortex of rats and mice exposed to normoxia (Nx) or hypoxia (Hx) 1, 7, or 21 days. Hypoxic acclimatization triggers a continuous increase of mitochondrial content (estimated through CS activity) in the retrosplenial cortex of rats during acclimatization to hypoxia (Hx). Maximum values, 800 % time normoxic control levels (Nx), are reached by day 21. Opposingly, in mice, mitochondrial volumes are reduced by 27 % after 21-day hypoxia (**A**). Similarly, the concentration of mitochondrial (**B**) and -to a less extent- cytosolic (**C**) proteins increase in rats while the opposite occurs in mice. $^{\#}p < 0.05$; $^{\#\#}p < 0.01$; and $^{\#\#\#\#}p < 0.0001$ vs. Nx control; $^{a*}p < 0.05$; and $^{a****}p < 0.0001$ vs. Hx 1d; $^{b*}p < 0.05$; $^{b**}p < 0.01$; and $^{b****}p < 0.0001$ vs. Hx 7d. n = 5–6.

Based on these results, we calculated the relative ATP synthesis and O_2 consumption (in the $OXPHOS_{NS}$ state) rates normalized to CS activity. In rats, the ATP/CS (Fig. 5A) ratio showed a bimodal pattern, with a first decline at day 1 and a second decline after 21 days, while the OCR/CS (Fig. 5B) ratio dropped only after 21 days. In mice, the efficiency of the ATP production normalized to mitochondrial mass (ATP/CS) increased quickly after 1-day acclimatization and remained elevated at 21 days after peaking at day 7. Contrastingly, after a peak at day 7, the OCR/CS dropped below normoxic levels by day 21.

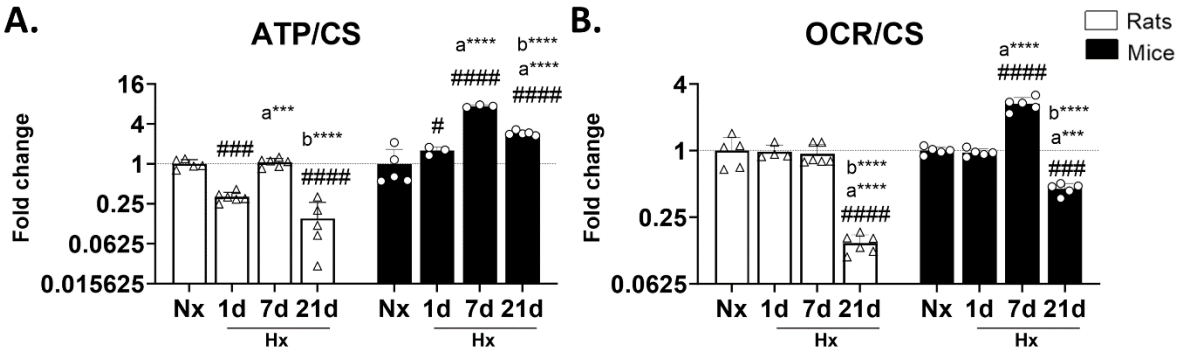

Figure 5. Relative ATP production (A) and oxygen consumption (B) rates normalized to citate synthase activity in the retrosplenial cortex of rats and mice exposed to normoxia (Nx) or hypoxia (Hx) 1, 7, or 21 days. Acclimatization to hypoxia significantly reduces the ATP synthesis and OCR in rats, while in mice ATP production is enhanced without increases in oxygen consumption. $^{\#\#}p < 0.01$; and $^{\#\#\#}p < 0.001$; $^{\#\#\#\#}p < 0.0001$ vs. Nx; $^{a**}p < 0.01$; and $^{a****}p < 0.0001$ vs. Hx 1d; $^{b*}p < 0.05$ vs. Hx 7d. n = 3–6.

3.5. Hypoxia-acclimatizing brain mitochondrial plasticity is not associated with the expression of genes involved in mitochondrial fission, fusion, or mitogenesis in mice

Since mitochondrial plasticity can arise form adjustments in mitochondrial bioenergetics (ATP production and O_2 consumption), dynamics (fusion, fission, mitogenesis, and mitophagy), and/or ultrastructure (size, shape, and cristae content) (Bennett, Latorre-Muro, & Puigserver, 2022; Tian, Zhang, Li, Wang, Li, & Zheng, 2020), we were interested in looking whether the relative bioenergetic enhancement we observed in mice was associated with modifications in mitochondrial dynamics and/or ultrastructure. For this, we quantified the mRNA expression levels of genes involved in the regulation of mitochondrial fission (dynamin-related protein 1 - DRP1, dynamin 2 - DNM2), fusion (mitofusins 1 and 2 - MFN1, MFN2), and mitogenesis (mitochondrial transcription factor A - TFAM, nuclear respiratory factor 1 - NRF1, peroxisome proliferator-activated receptor gamma coactivator 1α - PGC1α). We found divergent effects of hypoxia acclimatization in rats and mice in the relative expression of DRP1 (Two-way ANOVA $F_{species}$ = 0.132 d.f.= 1, 24; p=0.719; $F_{exposure}$ = 3.98; d.f.= 3, 24; p=0.02; $F_{species\_X\_exposure}$ = 4.19; d.f.= 3, 24; p=0.016), DNM2 (Two-way ANOVA $F_{species}$ = 0.339 d.f.= 1, 22; p=0.566; $F_{exposure}$ = 5.95; d.f.= 3, 22; p=0.004; $F_{species\_X\_exposure}$ = 4.65; d.f.= 3, 22; p=0.0115), MFN1 (Two-way ANOVA $F_{species}$ = 39.9 d.f.= 1, 24; p<0.0001; $F_{exposure}$ = 3.2; d.f.= 3, 24; p=0.041; $F_{species\_X\_exposure}$ = 8.96; d.f.= 3, 24; p=0.0004), MFN2 (Two-way ANOVA $F_{species}$ = 3.28 d.f.= 1, 24; p<0.083; $F_{exposure}$ = 1.52; d.f.= 3, 24; p=0.236; $F_{species\_X\_exposure}$ = 4.06; d.f.= 3, 24; p=0.018), TFAM (Two-way ANOVA $F_{species}$ = 2.81 d.f.= 1, 24; p=0.107; $F_{exposure}$ = 2.84; d.f.= 3, 24; p=0.059; $F_{species\_X\_exposure}$ = 8.11; d.f.= 3, 24; p=0.0007), and NRF1 (Two-way ANOVA $F_{species}$ = 1.91 d.f.= 1, 24; p=0.179; $F_{exposure}$ = 8.95; d.f.= 3, 24; p=0.0004; $F_{species\_X\_exposure}$ = 10.4; d.f.= 3, 24; p=0.0001). PGC1-α remained unaffected in both species (Two-way ANOVA $F_{species}$ = 2.03 d.f.= 1, 24; p=0.167; $F_{exposure}$ = 1.97; d.f.= 3, 24; p=0.414; $F_{species\_X\_exposure}$ = 0.577; d.f.= 3, 24; p=0.636). In rats, hypoxia increased the relative abundance of MFN1 (+50 %), TFAM (+21 %), and NRF1 (+46 %) transcripts in comparison with normoxic controls at 1-day exposure, however, after 7 days, mRNA levels of DRP1, DNM2, MFN1, MFN2, TFAM, and NRF1 dampened to around 50 - 70 % control values - Fig. 6A, B, C, D, E, F). Contrastingly, in mice, acclimatization to hypoxia enhanced the expression level of MFN1, reaching a 70 % increase at day 7 (Fig. 6C). These data suggest that whereas processes like fission, fusion, and mitogenesis which govern the dynamics of mitochondrial structural reconfiguration are importantly affected by hypoxic acclimatization in rats, they remain comparatively far less altered in mice.

Furthermore, transmission electron microscopy (TEM) analysis performed only in mice revealed that hypoxic acclimatization alters the mitochondrial abundance (One-way ANOVA F = 30 d.f.= 2, 147; p<0.0001), surface area (One-way ANOVA F = 3.52 d.f.= 2, 317; p=0.031), length (One-way ANOVA F = 8.11 d.f.= 2, 317; p=0.0004), and width (One-way ANOVA F = 4.58 d.f.= 2, 315; p=0.011), confirming the reduction of mitochondrial content at day 7 (Fig. 7A, B, C, D, E) and showing that mitochondria become more circular after 21 days (One-way ANOVA F = 4.28 d.f.= 2, 317; p=0.015 - Fig. 7F). Notwithstanding, while the cristae abundance (One-way ANOVA F = 8.77 d.f.= 2, 318; p=0.0002 - Fig. 7G) and area (One-way ANOVA F = 5.37 d.f.= 2, 317; p=0.005 - Fig. 7H) also reduce after 7 days, the cristae volume density inside each mitochondrion, a feature positively associated with bioenergetic capacity, is preserved (One-way ANOVA F = 0.821 d.f.= 2, 317; p=0.44 –

Fig. 7I). These findings suggest that mitochondrial plasticity in the retrosplenial cortex of mice involves bioenergetic and ultrastructural adjustments independently of fusion, fission, and mitogenesis.

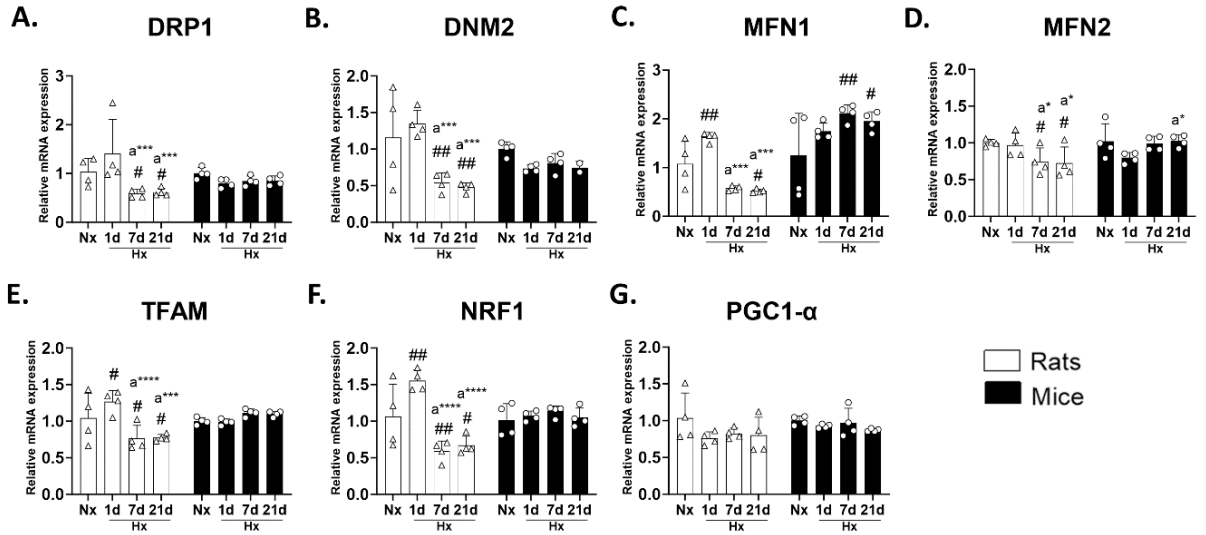

Figure 6. The relative mRNA expression of genes involved in mitochondrial fission (dynamin-related protein 1 – **A**, dynamin 2 – **B**), fusion (mitofusin 1 – **C**, mitofusin 2 - **D**), mitogenesis (mitochondrial transcription factor A – **E**, nuclear respiratory factor 1 – **F**, peroxisome proliferator-activated receptor gamma coactivator 1α - **G**) is significantly altered in rats while remains virtually unchanged in mice. $^{\#}p < 0.05$; and $^{\#\#}p < 0.01$; vs. Nx; $^{a*}p < 0.05$; and $^{a****}p < 0.0001$ vs. Hx 1d. n = 4.

3.6. The anaerobic metabolism is not affected during acclimatization to hypoxia in the brain of rats but it is transiently upregulated in mice.

The input of glycolysis and anaerobic and aerobic pathways to the cellular metabolism was assessed through the determination of the hexokinase (HK), lactate dehydrogenase (LDH), and pyruvate dehydrogenase (PDH) activities respectively (Table 6). Rats showed no significant response to hypoxic exposure in any of the studied enzymes. Conversely, the activities of HK (+33 % - Two-way ANOVA $F_{species}$ = 52.9 d.f.= 1, 39; p<0.001; $F_{exposure}$ = 4.16; d.f.= 3, 39; p=0.012; $F_{species\_X\_exposure}$ = 4.75; d.f.= 3, 39; p=0.006) and LDH (+600 % - Two-way ANOVA $F_{species}$ = 21.9 d.f.= 1, 37; p<0.001; $F_{exposure}$ = 58.9; d.f.= 3, 37; p<0.001; $F_{species\_X\_exposure}$ = 32.5; d.f.= 3, 37; p<0.001) were significantly enhanced in mice exposed to hypoxia for 7 days. Yet, in both cases, control levels were restored by day 21 (Fig. 8A, B). Noticeably, the PDH activity remained unaltered despite hypoxic exposure (Two-way ANOVA $F_{species}$ = 279 d.f.= 1, 24; p<0.001; $F_{exposure}$ = 2.75; d.f.= 3, 24; p = 0.065; $F_{species\_X\_exposure}$ = 1.84; d.f.= 3, 24; p = 0.168 - Fig. 8C).

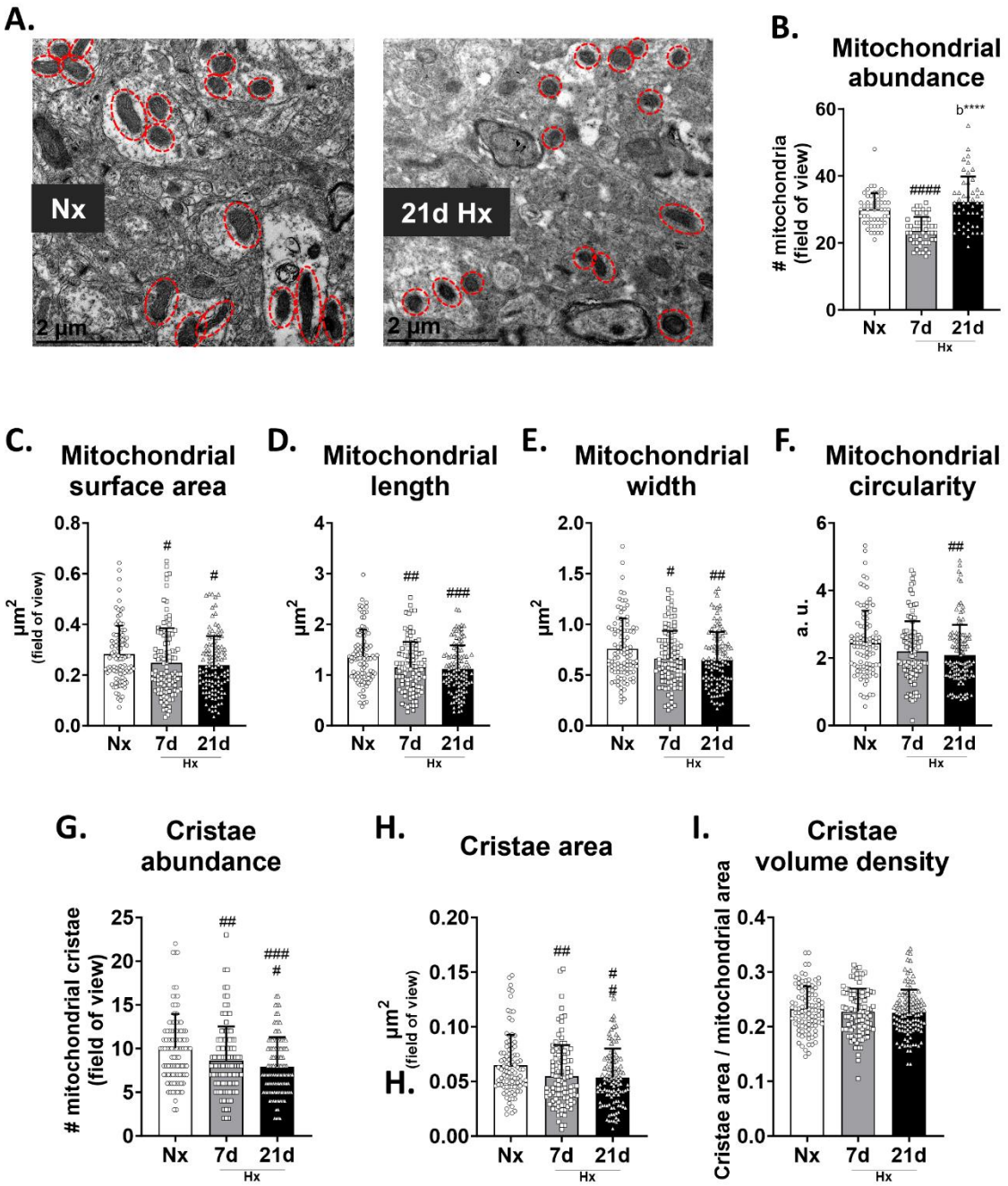

Figure 7. Acclimatization to hypoxia changes the ultrastructure and abundance of mitochondria in the retrosplenial cortex of mice (**A, B**), making them smaller (**C**, **D**, **E**) and more circular (**F**) but preserving the volume density of cristae (**G**, **H**, **I**). $^{\#}p < 0.05$; $^{\#\#}p < 0.01$; and $^{\#\#\#}p < 0.001$; vs. Nx; $^{b****}p < 0.0001$ vs. Hx 7d. n = 2.

Table 6. Enzymatic activity of hexokinase (HK), pyruvate dehydrogenase (PDH), and lactate dehydrogenase (LDH).

	Rats (mean ± S.D.)				Mice (mean ± S.D.)			
	Nx	**1 day Hx**	**7 days Hx**	**21 days Hx**	**Nx**	**1 day Hx**	**7 days Hx**	**21 days Hx**
HK (mIU/mg tissue)	4.73 ± 0.38	4.4 ± 0.29	4.34 ± 0.31	4.93 ± 0.2	38.88 ± 7.59	36.55 ± 2.29	51.84 ± 1.97	37.75 ± 1.82
LDH (mIU/mg tissue)	0.47 ± 0.09	0.44 ± 0.08	0.56 ± 0.21	0.4 ± 0.1	0.13 ± 0.03	0.12 ± 0.07	0.92 ± 0.05	0.14 ± 0.04
PDH (mOD/min)	0.29 ± 0.05	0.28 ± 0.06	0.29 ± 0.06	0.21 ± 0.04	0.86 ± 0.12	0.82 ± 0.08	0.67 ± 0.15	0.75 ± 0.07

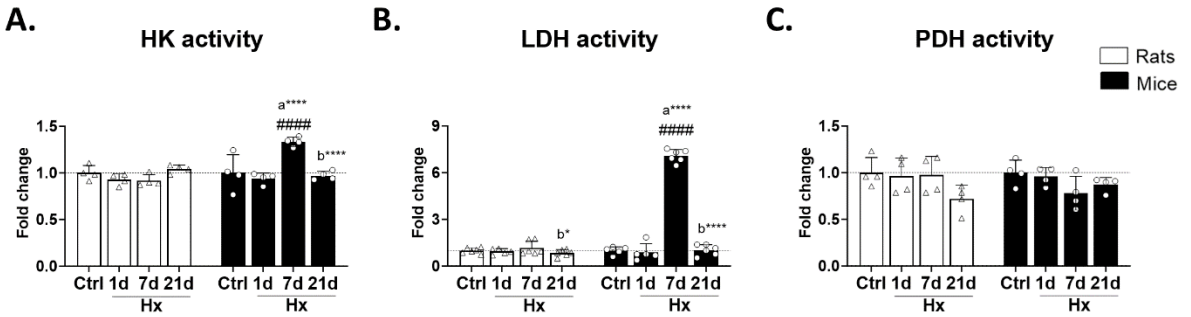

Figure 8. Activity of cellular metabolic pathways in the retrosplenial cortex of rats and mice exposed to normoxia (Nx) or hypoxia (Hx) for 1, 7, or 21 days. No changes occurred in any of the assessed metabolic pathways in rats regardless of hypoxic exposure. In mice, a transient upregulation of glycolysis (hexokinase activity – HK) at hypoxic day 7 (**A**) coincides with an equivalent upsurge in anaerobic metabolism (lactate dehydrogenase activity – LDH – **B**). These changes occur independently of aerobic metabolism (pyruvate dehydrogenase activity – PDH – **C**). #### $p < 0.0001$ vs. Nx; a**** $p < 0.0001$ vs. Hx 1d; b**** $p < 0.0001$ vs. Hx 7d. n = 4–6.

4. Discussion

The results presented here show that rats and mice exhibit major differences in their cellular and mitochondrial responses to hypoxic acclimatization in the retrosplenial cortex, a brain region that is critically important for spatial orientation and navigation, memory, and cognition. Both species show a swift increase in ATP synthesis and an overall improvement in ATP production efficiency (P»/O ratio). However, these adjustments are not maintained in rats, while they remain for at least 3 weeks of hypoxia in mice. Most strikingly, in rats, such responses are accompanied by a drastic elevation of mitochondrial mass (evidenced by increased CS activity and mitochondrial protein content) and altered mitochondrial dynamics, whereas mice sustained high P»/O ratios while decreasing mitochondrial mass and preserving the internal mitochondrial structure, ultimately contributing to reducing the overall oxygen consumption. These results suggest the existence of molecular mechanisms intended to enhance the coupling efficiency between oxidation and phosphorylation in mitochondria to ensure optimal tissue oxygenation while preserving ATP supply in the RSC of mice, which do not exist or are blunted in rats. Thus, our results reveal key clues to explain the differences between adaptive and non-adaptive brain metabolic acclimatization to hypoxia.

4.1. The "less oxygen, more ATP" paradox

The brain is highly dependent on oxygen and very sensitive to changes in its provision. This is illustrated by the fact that 90 % of the oxygen delivered to this organ is immediately used for energy production since cerebral cells have high basal energy requirements and are virtually incapable of keeping energy reserves (L Lukyanova, 1997). Moreover, the retrosplenial area of the cortex is particularly sensitive to hypoxia and reacts quickly to alterations in oxygen availability (Kleszka et al., 2020; Sharp, Bergeron, & Bernaudin, 2001). Traditionally, it has been suggested that under hypoxic conditions, animals react by acutely reducing their overall metabolic demand

(hypometabolism) and/or increasing anaerobic metabolic rates to preserve energy homeostasis (Ramirez, Folkow, & Blix, 2007). Although these responses appear plausible in the short term, both strategies are likely impractical under chronic hypoxia such as that sustained by high-altitude settlers, and it appears reasonable to postulate that cerebral hypometabolism would be unfavorable to cognitive function while the considerably slower rates for synthesizing ATP of glycolysis compared to aerobic phosphorylation look incompatible with brain requirements in the long term (Erecińska & Silver, 2001; Ramirez, Folkow, & Blix, 2007). Thus, mechanisms that allow more effective management of oxygen and ATP production shall exist in such species. Our data strongly suggest that oxygen economy does not necessarily imply hypometabolism nor persistent upregulation of anaerobic pathways. Here we show that the overall ATP production rates increase in both rats and mice upon hypoxic exposure, while the anaerobic metabolism is only momentarily elevated exclusively in mice. In rats, the transient increase of ATP production may be explained by the corresponding rise in mitochondrial content. On the other hand, in mice, the optimized ATP synthesis does not involve higher mitochondrial mass or oxygen consumption. Considering that the overall plastic mitochondrial response to hypoxia is governed by adjustments in mitochondrial bioenergetics (ETS efficiency), mitochondrial dynamics (fusion, fission, mitogenesis, and mitophagy), and mitochondrial ultrastructure (Bennett, Latorre-Muro, & Puigserver, 2022; Tian et al., 2020); our findings suggest that in rats, the expression of mitochondrial plasticity during hypoxic acclimatization is subordinated to the augmentation of mitochondrial content and reduced expression of mechanisms governing mitochondrial fission and fusion, while in mice mitochondria, it entails fission-and-fusion-independent adjustments in the ultrastructure which preserve the internal configuration of cristae and accompany the regulation —and possibly the reconfiguration— of the ETS functioning to promote an enhanced coupling between oxidation and phosphorylation. This implies that in normoxia, as suggested before (M. Brand, 2005; Gnaiger, 2001), the efficiency of one or both these processes is suboptimal, likely due to the wasteful effects of electron slippage from the ETS and the leak of protons through the inner mitochondrial membrane. Interestingly, it has been shown recently that chronic exposure to physiological levels of hypoxia minimizes the electron slippage in cultures of brain tissue of mice as a consequence of the diminished electron flux through Complex III (Spinelli et al., 2021). The mechanism behind such adjustment involves the net reversion of the activity of succinate dehydrogenase (SDH – Complex II), causing the chemical reduction of fumarate into succinate. Under these circumstances, not only the involvement of the S pathway in the ETS' OCR is significantly depressed, but an important fraction of the electrons coming from NADH (N pathway) are sequestrated by SDH and flow toward fumarate instead of oxygen -avoiding Complex III. Then, the newly formed succinate will re-enter the TCA cycle enabling NADH reoxidation and privileging the proton export by Complex I over complexes III and IV while reducing oxygen use (Spinelli et al., 2021). Concurrently, hypoxia also produces a decrease in proton leak because of the shortened redox span of the ETS (which averts the membrane potential from reaching levels that would force protons through the inner mitochondrial membrane into the matrix), and the reduced ion permeability of the mitochondrial membrane (M. D. Brand, Chien, Ainscow, Rolfe, & Porter, 1994; Canton, Luvisetto, Schmehl, & Azzone, 1995; Gnaiger, Méndez, & Hand, 2000; Jones, 1995; Mitchell & Moyle, 1967). Our results in OXPHOS and LEAK respiration, and ETS maximum capacity clearly support the hypothesis that these mechanisms

explain, at least in part, the sustained higher efficiency of ATP production under chronic hypoxia in mice (Fig. 9).

Stoichiometrically, the efficiency of the ETS is classically expressed as the number of ATP molecules synthesized per atomic oxygen reduced by CIV, namely the P»/O ratio. According to the chemiosmotic theory, the P»/O can be calculated as the ratio of H^+ exported into the intermembrane space per atom of oxygen reduced (H^+/O), and the H^+ imported (i.e. by the ATP synthase + adenine nucleotide and phosphate carriers) per molecule of ATP synthesized (H^+/P») (Nath, 2019). Remarkably, in hypoxia, since fumarate acts as a second terminal electron acceptor (Spinelli et al., 2021), the H^+/fumarate reduced relation will directly augment the P»/O ratio. Indeed, in line with our findings, Gnaiger, Méndez, and Hand (2000) found a 4.5-fold increase in the ADP/O ratio (equivalent to P»/O) in isolated mitochondria from rat liver and the anoxia-tolerant embryo of the brine shrimp, *Artemia franciscana*, studied under hypoxic conditions. Nonetheless, it should be noted that here we report high P»/O ratios that are seemingly incompatible with traditionally accepted maximal values (N pathway = 2.73; S pathway = 1.64 (Salin et al., 2016; Watt, Montgomery, Runswick, Leslie, & Walker, 2010)). While we cannot rule out that our values are overestimated, it is also notable that the stoichiometry of ATP production per oxygen used depends on the integral assembly and functioning of the ETS, which is increasingly accepted to be different under hypoxia (Feala, Coquin, Zhou, Haddad, Paternostro, & McCulloch, 2009; Fuhrmann & Brüne, 2017; Gnaiger, 2001; Gnaiger, Méndez, & Hand, 2000; Pamenter, Lau, Richards, & Milsom, 2018). Indeed, all the traditional estimates of P»/O consider oxygen as the only terminal electron acceptor possible disregarding the newly found role of succinate. In this context and considering that the P»/O ratios we obtained for normoxic controls are consistent with classical theoretical values, our data support the notion that the stoichiometry of O_2 consumption, electron transfer, H^+ export, ADP utilization, and ATP production within the ETS is different under chronic hypoxic conditions compared to that described in normoxia for brain mitochondria. Interestingly, enhanced efficiency of ATP synthesis has been consistently suggested in hypoxia-adapted/acclimatized mammals as in invertebrates, pointing to a general adaptive bioenergetic response to environmental hypoxia (Feala et al., 2009; Gnaiger, 2001; Gnaiger, Méndez, & Hand, 2000; Hochachka, Buck, Doll, & Land, 1996; LD Lukyanova, Germanova, Tsybina, & Chernobaeva, 2009; Ludmila D. Lukyanova & Kirova, 2015; L. D. Lukyanova, Romanova, & Chernobaeva, 1991; Reynafarje & Marticorena, 2002; Zungu, Young, Stanley, & Essop, 2008).

4.2. Is the downregulation of oxygen consumption in brain mitochondria an adaptive oxygen-saving strategy to face chronic hypoxia?

Reducing oxygen consumption in brain cells upon hypoxic exposure has been reported extensively (Buck & Pamenter, 2006; Erecińska & Silver, 2001; Ludmila D. Lukyanova & Kirova, 2015; Ramirez, Folkow, & Blix, 2007), and while this has been traditionally interpreted as a sign of hypometabolism, our present data show that mice can sustain high ATP synthesis rates in the brain while decreasing their oxygen consumption. This is especially relevant when considering that successful cerebral responses to hypoxia should integrate metabolic regulation and functional integrity (Ramirez, Folkow, & Blix, 2007). We observed that in rats, acclimatization to hypoxia promotes a temporary increase of mitochondrial respiration, linked to increased activity of the succinate-dependent S pathway (Fig. 3). Such response has been reported

previously in the brain cortex of albino rats subjected chronically to different levels of hypoxia (8 – 14 % O_2) (L Lukyanova, 1997; LD Lukyanova, Dudchenko, Tzybina, & Germanova, 2008; Ludmila D. Lukyanova & Kirova, 2015; L. D. Lukyanova, Kirova, & Germanova, 2018), in association with a temporary inhibition of the activity of the N-pathway, which we did not observe. As in our work, both pathways are restored at later stages of hypoxic exposure. Conversely, in Wistar rats, the respiration of brain-cortex mitochondria remains unaffected after 1 month of hypobaric hypoxia (404 torr ≈ 5,000 m) (Czerniczyniec, La Padula, Bustamante, Karadayian, Lores-Arnaiz, & Costa, 2015), however, no data is presented for the first four weeks of exposure. Even if transitory, an overall upregulation in mitochondrial respiration under hypoxic conditions is puzzling and may imply detrimental imbalances in the homeostasis of oxygen at the cerebral level. Indeed, it has been shown in models of cerebrovascular accident (ischemia-reperfusion) that when the cerebral blood flow and oxygen supply are reduced, but the cellular oxygen consumption remains unchanged, the cells proximal to capillaries may deplete the limited oxygen provided, thus, causing severe hypoxia or anoxia in more distal regions (i.e., hypoxic penumbra), promoting apoptosis, and ultimately affecting brain function (Czerniczyniec et al., 2015; Erecińska & Silver, 2001; Ledo, Barbosa, Cadenas, & Laranjinha, 2010). For the retrosplenial cortex, this would imply altered spatial orientation and navigation, memory, and cognition (Milczarek & Vann, 2020; Nelson, Powell, Holmes, Vann, & Aggleton, 2015; Vann, Aggleton, & Maguire, 2009). In effect, Long-Evans rats exhibit neuronal apoptosis with detrimental effects on spatial cognition within ten days of housing at an altitude of 3,450 m (Koester-Hegmann et al., 2019). In the SD rats that we used here, after 21 days of hypoxic exposure, the initially increased mitochondrial oxygen consumption is brought back to control levels likely by the inhibition of CIV (Fig. 3E), and it might be speculated that this helps to prevent further aggravation in brain functions. This response has been suggested to be regulated by a hypoxia-induced elevated synthesis of NO, which acts as an allosteric competitor of oxygen, and effectively reduces mitochondrial respiration (Brunori, Giuffrè, Forte, Mastronicola, Barone, & Sarti, 2004; Ricardo Cáceda, Gamboa, Boero, Monge-C, & Arregui, 2001; Juan C Chávez, Agani, Pichiule, & LaManna, 2000; Czerniczyniec et al., 2015; Galkin, Higgs, & Moncada, 2007; Hagen, Taylor, Lam, & Moncada, 2003; Solaini, Baracca, Lenaz, & Sgarbi, 2010).

Contrastingly, in mice, normoxia-like levels of mitochondrial respiration are well preserved during the first week of hypoxic exposure followed by a clear drop after 21 days. Identically, OXPHOS and LEAK respiration are depressed in mitochondria isolated from the brain cortex of Balb/c mice exposed to three-week hypobaric hypoxia (455 torr ≈ 4,200 m) (Juan Carlos Chávez, Pichiule, Boero, & Arregui, 1995). In our animals, this downregulation is associated with reduced activity of the S pathway (see Fig. 2D and 3D) and occurs independently of changes in mitochondrial content. In this context, the accumulation of succinate in the brain of mice upon chronic hypoxic exposure that has been consistently reported over the years appears coherent (R Cáceda, Boero, & Arregui, 1997; Ricardo Cáceda et al., 2001; Sahni et al., 2018; Zhang et al., 2022). As discussed above, recent data have shown that physiological levels of hypoxia induce the net reversion of the enzymatic activity of cerebral SDH causing the chemical reduction of fumarate into succinate. In this scenario, fumarate takes electrons away from oxygen, and consequently, the mitochondrial use of oxygen decreases, albeit without necessarily affecting the synthesis of ATP (Spinelli et al., 2021). Interestingly, oxygen economy linked to decreased overall ETS flux is common in the brain of species that are considered to be

well adapted to hypoxia such as "hypoxia high-resistant" lab rats, naked mole-rats, and red-eared slider turtles, suggesting that this constitutes an adaptive trait for life in oxygen-limited environments (Buck & Pamenter, 2006; Dudchenko, Chernobaeva, Belousova, Vlasova, & Luk'yanova, 1993; LD Lukyanova, Dudchenko, et al., 2009; L. D. Lukyanova, Germanova, & Kopaladze, 2009; Ludmila D. Lukyanova & Kirova, 2015; L. D. Lukyanova, Romanova, & Chernobaeva, 1991; Pamenter, Gomez, Richards, & Milsom, 2016; Pamenter et al., 2018).

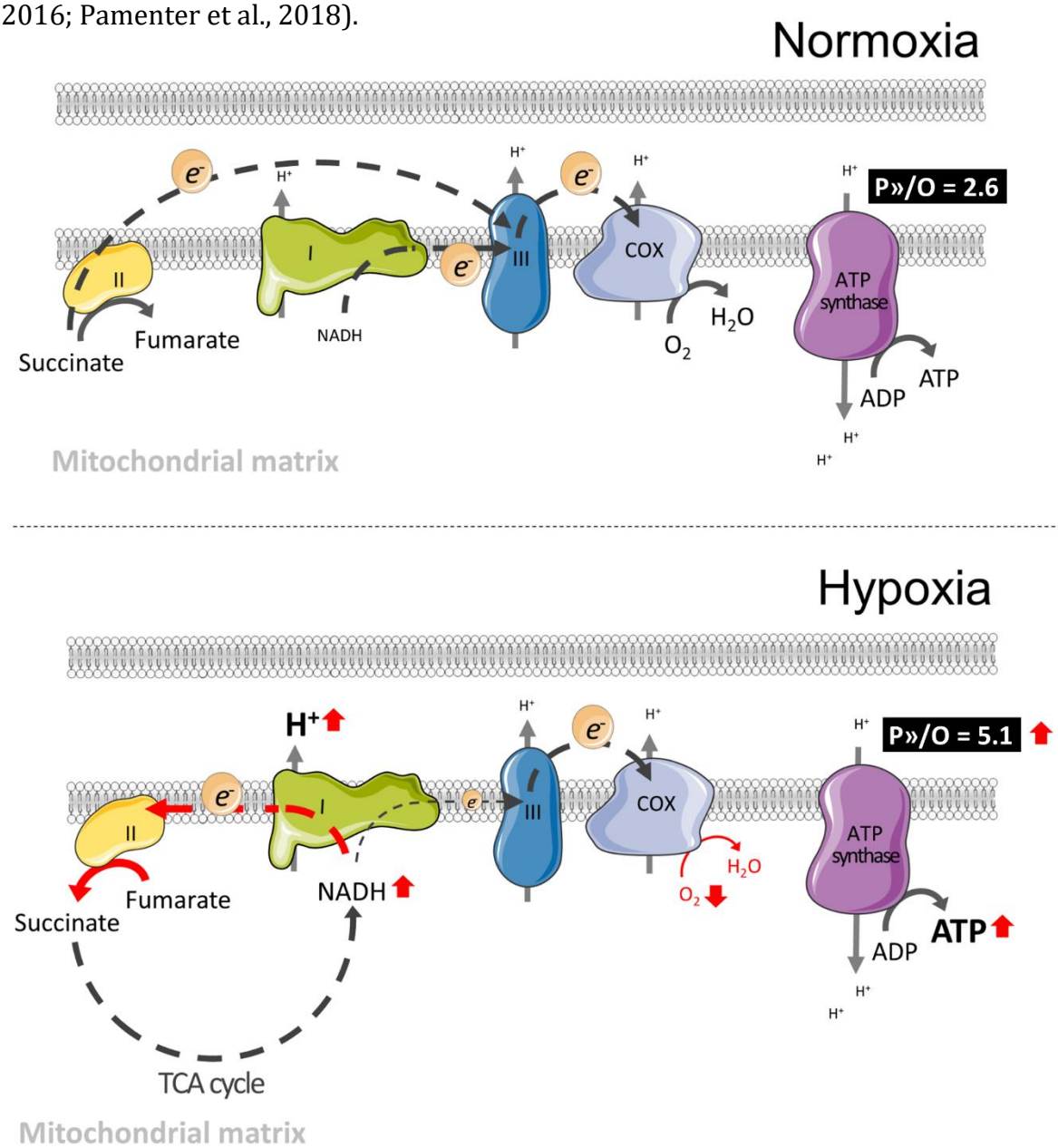

Figure 9. Increases in P»/O ratio during acclimatization to hypoxia can be explained by a new circuitry in the ETS that uses fumarate as alternate terminal electron acceptor deputizing for oxygen due to the net reversion of the activity of Complex II (Spinelli et al., 2021). In these conditions, electrons quickly return to the TCA cycle and are recycled, in consequence, proton export by Complex I is enhanced compared to normoxic conditions while membrane potential and ATP synthesis are sustained or even enhanced. Ultimately, oxygen consumption is reduced. Altered factors in the ETS are marked in red. Red arrows indicate changes (increase, decrease, or direction of the reaction).

4.3. Is cell-and-mitochondrial metabolic plasticity the ultimate key to successful acclimatization to high altitude in mice?

Finetuning the metabolic activity at the cellular and mitochondrial levels to improve the efficiency of oxygen utilization and energy production likely underlies adaptation to low-oxygen environments in species living at altitude. Conversely, when non-adapted species face hypoxia these mechanisms are somehow limited or impaired, and may ultimately affect their ability to successfully colonize these habitats (Dawson, Alza, Nandal, Scott, & McCracken, 2020; Lalejini, Ferguson, Grant, & Ofria, 2021). We have shown previously that in addition to -allegedly adaptive- adjustments in ventilation, oxygen transport, and whole-body metabolism, the bioenergetic maximum capacity of liver mitochondria increases in mice during acclimatization to hypoxia in an S-pathway-dependent manner, while this response is absent in rats (Christian Arias-Reyes, Soliz, & Joseph, 2021). Here we show that in the retrosplenial cortex, contrary to the liver, declining mitochondrial respiration appears to be the adaptive norm. Moreover, it is remarkable that as in hepatic mitochondria, this plastic response is associated with the modulation of the S pathway, supporting the hypothesis of the key role of succinate, and SDH, in metabolic adaptation/acclimatization to hypoxia (Dawson et al., 2020; Fuhrmann & Brüne, 2017; Ludmila D. Lukyanova & Kirova, 2015; Spinelli et al., 2021). On the other hand, while mitochondrial plasticity does exist in the retrosplenial cortex of rats, it is expressed differently and increased mitochondrial biogenesis appears necessary to cope with chronic hypoxia, presumably requiring high amounts of energy for synthesis and transport of proteins. Under these circumstances, one might hypothesize that metabolically demanding tasks, like physical or cognitive efforts, should be challenging and likely compromise cognition or other brain functions (Dudchenko et al., 1993; L. D. Lukyanova, Germanova, & Kopaladze, 2009). In this scenario, biological fitness shall get severely affected, and ultimately, this may explain, at least in part, why common rats are virtually absent at high altitudes (Christian Arias-Reyes, Soliz, & Joseph, 2021; Jochmans-Lemoine et al., 2016; Jochmans-Lemoine et al., 2015). In summary, notwithstanding the optimized configuration at system, organ, and tissue levels, that is present in mice, it might be argued that the mitochondrial adjustments reported here are the major determinants of the adaptive acclimatizing response to hypoxia and may greatly affect their success in colonizing high-altitude environments.

5. Conclusion

We conclude that acclimatization to hypoxia triggers divergent metabolic plasticity at the cellular and mitochondrial levels in the retrosplenial cortex of SD rats and FVB mice. While in rats this response involves energetically expensive increases in mitochondrial content and adjustments in mitochondrial dynamics to compensate for poorly efficient mitochondria, in mice it comprises a more conservative use of oxygen and the enhancement of ETS-operating and ATP-production efficiencies, implying the protection of spatial memory and cognition, and ultimately, biological fitness. The absence of such adjustments may conceivably be detrimental to the ability to cope with environmental hypoxia and thus colonizing high-altitude habitats. Altogether, these findings support the hypothesis of house mice being pre-adapted to hypoxia and help to explain the absence of common rats in high-altitude regions.

Acknowledgements

This study was funded by the Natural Sciences and Engineering Council of Canada (NSERC RGPIN-2019-06495 to VJ). CA-R received Ph. D. scholarships from the "Reseau de Santé Respiratoire du Québec" and the "Fonds de Recherche du Québec- Santé" (292950). JS is supported by the "Fonds de recherché du Québec-Santé" (FRQ-S; FQ121919). VJ and JS are members of the "Physiological breathing disorders" axis of the Quebec Respiratory Health Network.

References

Arias-Reyes, C., Losantos-Ramos, K., Gonzales, M., Furrer, D., & Soliz, J. (2019). NADH-linked mitochondrial respiration in the developing mouse brain is sex-, age- and tissue-dependent. *Respiratory physiology & neurobiology, 266*, 156-162. doi:https://doi.org/10.1016/j.resp.2019.05.011

Arias-Reyes, C., Soliz, J., & Joseph, V. (2021). Mice and Rats Display Different Ventilatory, Hematological, and Metabolic Features of Acclimatization to Hypoxia. *Frontiers in Physiology, 12*(265). doi:10.3389/fphys.2021.647822

Bennett, C. F., Latorre-Muro, P., & Puigserver, P. (2022). Mechanisms of mitochondrial respiratory adaptation. *Nature Reviews Molecular Cell Biology, 23*(12), 817-835. doi:10.1038/s41580-022-00506-6

Bonhomme, F., & Searle, J. B. (2012). House mouse phylogeography. In S. J. E. B. Miloš Macholán, Pavel Munclinger and Jaroslav Piálek (Ed.), *Evolution of the house mouse* (Vol. 3, pp. 278). Cambridge, UK: Cambridge University Press.

Brand, M. (2005). The efficiency and plasticity of mitochondrial energy transduction. *Biochemical Society Transactions, 33*(5), 897-904.

Brand, M. D., Chien, L.-F., Ainscow, E. K., Rolfe, D. F. S., & Porter, R. K. (1994). The causes and functions of mitochondrial proton leak. *Biochimica et Biophysica Acta (BBA) - Bioenergetics, 1187*(2), 132-139. doi:https://doi.org/10.1016/0005-2728(94)90099-X

Brunori, M., Giuffrè, A., Forte, E., Mastronicola, D., Barone, M. C., & Sarti, P. (2004). Control of cytochrome *c* oxidase activity by nitric oxide. *Biochimica et Biophysica Acta (BBA) - Bioenergetics, 1655*, 365-371. doi:https://doi.org/10.1016/j.bbabio.2003.06.008

Buck, L. T., & Pamenter, M. E. (2006). Adaptive responses of vertebrate neurons to anoxia—Matching supply to demand. *Respiratory physiology & neurobiology, 154*(1), 226-240. doi:https://doi.org/10.1016/j.resp.2006.03.004

Cáceda, R., Boero, J., & Arregui, A. (1997). Increase in succinate dehydrogenase activity in mice brain during chronic hypoxia. *Acta andin, 6*(2), 142-144.

Cáceda, R., Gamboa, J. L., Boero, J. A., Monge-C, C., & Arregui, A. (2001). Energetic metabolism in mouse cerebral cortex during chronic hypoxia. *Neuroscience letters, 301*(3), 171-174.

Canton, M., Luvisetto, S., Schmehl, I., & Azzone, G. F. (1995). The nature of mitochondrial respiration and discrimination between membrane and pump properties. *Biochemical Journal, 310*(2), 477-481. doi:10.1042/bj3100477

Chávez, J. C., Agani, F., Pichiule, P., & LaManna, J. C. (2000). Expression of hypoxia-inducible factor-1α in the brain of rats during chronic hypoxia. *Journal of Applied Physiology, 89*(5), 1937-1942.

Chávez, J. C., Pichiule, P., Boero, J., & Arregui, A. (1995). Reduced mitochondrial respiration in mouse cerebral cortex during chronic hypoxia. *Neuroscience letters, 193*(3), 169-172. doi:https://doi.org/10.1016/0304-3940(95)11692-P

Chinopoulos, C., Kiss, G., Kawamata, H., & Starkov, A. A. (2014). Chapter Seventeen - Measurement of ADP–ATP Exchange in Relation to Mitochondrial Transmembrane Potential and Oxygen Consumption. In L. Galluzzi & G. Kroemer (Eds.), *Methods in Enzymology* (Vol. 542, pp. 333-348): Academic Press.

Czerniczyniec, A., La Padula, P., Bustamante, J., Karadayian, A., Lores-Arnaiz, S., & Costa, L. (2015). Mitochondrial function in rat cerebral cortex and hippocampus after short- and long-term hypobaric hypoxia. *Brain research, 1598*, 66-75.

Dawson, N. J., Alza, L., Nandal, G., Scott, G. R., & McCracken, K. G. (2020). Convergent changes in muscle metabolism depend on duration of high-altitude ancestry across Andean waterfowl. *Elife, 9*, e56259.

Doerrier, C., Garcia-Souza, L. F., Krumschnabel, G., Wohlfarter, Y., Mészáros, A. T., & Gnaiger, E. (2018). High-Resolution FluoRespirometry and OXPHOS Protocols for Human Cells, Permeabilized Fibers from Small Biopsies of Muscle, and Isolated Mitochondria. In C. M. P. a. A. J. Moreno (Ed.), *Mitochondrial Bioenergetics* (pp. 31-70): Springer.

Dudchenko, A. M., Chernobaeva, G. N., Belousova, V. V., Vlasova, I. G., & Luk'yanova, L. D. (1993). Bioenergetic parameters of the brain in rats with different resistance to hypoxia. *Bulletin of Experimental Biology and Medicine, 115*(3), 263-267. doi:10.1007/BF00836406

Erecińska, M., & Silver, I. A. (2001). Tissue oxygen tension and brain sensitivity to hypoxia. *Respiration physiology, 128*(3), 263-276. doi:https://doi.org/10.1016/S0034-5687(01)00306-1

Feala, J. D., Coquin, L., Zhou, D., Haddad, G. G., Paternostro, G., & McCulloch, A. D. (2009). Metabolism as means for hypoxia adaptation: metabolic profiling and flux balance analysis. *BMC Systems Biology, 3*(1), 91. doi:10.1186/1752-0509-3-91

Fuhrmann, D. C., & Brüne, B. (2017). Mitochondrial composition and function under the control of hypoxia. *Redox biology, 12*, 208-215.

Galkin, A., Higgs, A., & Moncada, S. (2007). Nitric oxide and hypoxia. *Essays in Biochemistry, 43*, 29-42. doi:10.1042/bse0430029

Gnaiger, E. (2001). Bioenergetics at low oxygen: dependence of respiration and phosphorylation on oxygen and adenosine diphosphate supply. *Respiration physiology, 128*(3), 277-297. doi:https://doi.org/10.1016/S0034-5687(01)00307-3

Gnaiger E - MitoEAGLE Task Group (2020) Mitochondrial physiology. Bioenerg Commun 2020.1. https://doi.org/10.26124/bec:2020-0001.v1

Gnaiger, E., Méndez, G., & Hand, S. C. (2000). High phosphorylation efficiency and depression of uncoupled respiration in mitochondria under hypoxia. *Proceedings of the National Academy of Sciences, 97*(20), 11080-11085. doi:doi:10.1073/pnas.97.20.11080

Hagen, T., Taylor, C. T., Lam, F., & Moncada, S. (2003). Redistribution of Intracellular Oxygen in Hypoxia by Nitric Oxide: Effect on HIF1α. *Science, 302*(5652), 1975-1978. doi:10.1126/science.1088805

Hochachka, P., Buck, L., Doll, C., & Land, S. (1996). Unifying theory of hypoxia tolerance: molecular/metabolic defense and rescue mechanisms for surviving oxygen lack.

Proceedings of the National Academy of Sciences, 93(18), 9493-9498. Retrieved from https://www.ncbi.nlm.nih.gov/pubmed/8790358

Jochmans-Lemoine, A., Revollo, S., Villalpando, G., Valverde, I., Gonzales, M., Laouafa, S., . . . Joseph, V. (2018). Divergent Mitochondrial Antioxidant Activities and Lung Alveolar Architecture in the Lungs of Rats and Mice at High Altitude. *Frontiers in Physiology, 9*(311). doi:10.3389/fphys.2018.00311

Jochmans-Lemoine, A., Shahare, M., Soliz, J., & Joseph, V. (2016). HIF1α and physiological responses to hypoxia are correlated in mice but not in rats. *Journal of Experimental Biology, 219*(24), 3952-3961.

Jochmans-Lemoine, A., Villalpando, G., Gonzales, M., Valverde, I., Soria, R., & Joseph, V. (2015). Divergent physiological responses in laboratory rats and mice raised at high altitude. *Journal of Experimental Biology, 218*(7), 1035-1043.

Jones, D. P. (1995). Mitochondrial dysfunction during anoxia and acute cell injury. *Biochimica et Biophysica Acta (BBA) - Molecular Basis of Disease, 1271*(1), 29-33. doi:https://doi.org/10.1016/0925-4439(95)00006-P

Kleszka, K., Leu, T., Quinting, T., Jastrow, H., Pechlivanis, S., Fandrey, J., & Schreiber, T. (2020). Hypoxia-inducible factor-2α is crucial for proper brain development. *Scientific Reports, 10*(1), 19146. doi:10.1038/s41598-020-75838-4

Koester-Hegmann, C., Bengoetxea, H., Kosenkov, D., Thiersch, M., Haider, T., Gassmann, M., & Schneider Gasser, E. M. (2019). High-Altitude Cognitive Impairment Is Prevented by Enriched Environment Including Exercise via VEGF Signaling. *Frontiers in Cellular Neuroscience, 12*. doi:10.3389/fncel.2018.00532

Lalejini, A., Ferguson, A. J., Grant, N. A., & Ofria, C. (2021). Adaptive Phenotypic Plasticity Stabilizes Evolution in Fluctuating Environments. *Frontiers in Ecology and Evolution, 9*. doi:10.3389/fevo.2021.715381

Ledo, A., Barbosa, R., Cadenas, E., & Laranjinha, J. (2010). Dynamic and interacting profiles of ·NO and O2 in rat hippocampal slices. *Free Radical Biology and Medicine, 48*(8), 1044-1050. doi:https://doi.org/10.1016/j.freeradbiomed.2010.01.024

Lukyanova, L. (1997). Bioenergy hypoxia: concept, mechanisms, correction. *Bull. Exp. Biol. Med, 124*, 244-254.

Lukyanova, L., Dudchenko, A., Germanova, E., Tsybina, T., Kopaladse, R., Ehrenbourg, I., & Tkatchouk, E. (2009). Mitochondrial signaling in formation of body resistance to hypoxia. *Intermittent hypoxia: from molecular mechanisms to clinical applications. New York: Nova*, 391-417.

Lukyanova, L., Dudchenko, A., Tzybina, T., & Germanova, E. (2008). Mitochondrial Signaling in Adaptation to Hypoxia. In N. T. L. Lukyanova, and P.K. Singai (Ed.), *Adaptation Biology and Medicine:* (Vol. 5, pp. 245). New Delhi, India: Narosa Publishing House.

Lukyanova, L., Germanova, E., Tsybina, T., & Chernobaeva, G. (2009). Energotropic effect of succinate-containing derivatives of 3-hydroxypyridine. *Bulletin of Experimental Biology and Medicine, 148*(4), 587-591.

Lukyanova, L. D., Germanova, E. L., & Kopaladze, R. A. (2009). Development of Resistance of an Organism under Various Conditions of Hypoxic Preconditioning: Role of the Hypoxic Period and Reoxygenation. *Bulletin of Experimental Biology and Medicine, 147*(4), 400. doi:10.1007/s10517-009-0529-8

Lukyanova, L. D., & Kirova, Y. I. (2015). Mitochondria-controlled signaling mechanisms of brain protection in hypoxia. *Frontiers in Neuroscience, 9*(320). doi:10.3389/fnins.2015.00320

Lukyanova, L. D., Kirova, Y. I., & Germanova, E. L. (2018). The Role of Succinate in Regulation of Immediate HIF-1α Expression in Hypoxia. *Bulletin of Experimental Biology and Medicine, 164*(3), 298-303. doi:10.1007/s10517-018-3976-2

Lukyanova, L. D., Romanova, V. E., & Chernobaeva, G. N. (1991). Oxidative phosphorylation in brain mitochondria of rats differing in their sensitivity to hypoxia. *Bulletin of Experimental Biology and Medicine, 112*(1), 962-965. doi:10.1007/BF00841143

Milczarek, M. M., & Vann, S. D. (2020). The retrosplenial cortex and long-term spatial memory: from the cell to the network. *Current Opinion in Behavioral Sciences, 32*, 50-56. doi:https://doi.org/10.1016/j.cobeha.2020.01.014

Mitchell, P., & Moyle, J. (1967). Respiration-driven proton translocation in rat liver mitochondria. *Biochemical Journal, 105*(3), 1147-1162. doi:10.1042/bj1051147

Nath, S. (2019). Integration of demand and supply sides in the ATP energy economics of cells. *Biophysical Chemistry, 252*, 106208. doi:https://doi.org/10.1016/j.bpc.2019.106208

Nelson, A. J. D., Powell, A. L., Holmes, J. D., Vann, S. D., & Aggleton, J. P. (2015). What does spatial alternation tell us about retrosplenial cortex function? *Frontiers in Behavioral Neuroscience, 9*(126). doi:10.3389/fnbeh.2015.00126

Pamenter, M. E., Gomez, C. R., Richards, J. G., & Milsom, W. K. (2016). Mitochondrial responses to prolonged anoxia in brain of red-eared slider turtles. *Biology Letters, 12*(1), 20150797. doi:doi:10.1098/rsbl.2015.0797

Pamenter, M. E., Lau, G. Y., Richards, J. G., & Milsom, W. K. (2018). Naked mole rat brain mitochondria electron transport system flux and H^+ leak are reduced during acute hypoxia. *Journal of Experimental Biology, 221*(4). doi:10.1242/jeb.171397

Ramirez, J.-M., Folkow, L. P., & Blix, A. S. (2007). Hypoxia Tolerance in Mammals and Birds: From the Wilderness to the Clinic. *Annual Review of Physiology, 69*(1), 113-143. doi:10.1146/annurev.physiol.69.031905.163111

Reynafarje, B. D., & Marticorena, E. (2002). Bioenergetics of the Heart at High Altitude: Environmental Hypoxia Imposes Profound Transformations on the Myocardial Process of ATP Synthesis. *Journal of bioenergetics and biomembranes, 34*(6), 407-412. doi:10.1023/A:1022597523483

Riedel, G., Düker, U., Fekete-Drimusz, N., Manns, M., Vondran, F., & Bock, M. (2014). An Extended ΔCT-Method Facilitating Normalisation with Multiple Reference Genes Suited for Quantitative RT-PCR Analyses of Human Hepatocyte-Like Cells. *PloS one, 9*, e93031. doi:10.1371/journal.pone.0093031

Sahni, P. V., Zhang, J., Sosunov, S., Galkin, A., Niatsetskaya, Z., Starkov, A., . . . Ten, V. S. (2018). Krebs cycle metabolites and preferential succinate oxidation following neonatal hypoxic-ischemic brain injury in mice. *Pediatr Res, 83*(2), 491-497. doi:10.1038/pr.2017.277

Salin, K., Villasevil, E. M., Auer, S. K., Anderson, G. J., Selman, C., Metcalfe, N. B., & Chinopoulos, C. (2016). Simultaneous measurement of mitochondrial respiration and ATP production in tissue homogenates and calculation of effective P/O ratios. *Physiological reports, 4*(20), e13007. doi:10.14814/phy2.13007

Sharp, F. R., Bergeron, M., & Bernaudin, M. (2001). Hypoxia-inducible factor in brain. In R. C. Roach, P. D. Wagner, & P. H. Hackett (Eds.), *Hypoxia: From Genes to the Bedside* (pp. 273-291). Boston, MA: Springer US.

Solaini, G., Baracca, A., Lenaz, G., & Sgarbi, G. (2010). Hypoxia and mitochondrial oxidative metabolism. *Biochimica et Biophysica Acta (BBA)-Bioenergetics, 1797*(6-7), 1171-1177.

Spinelli, J. B., Rosen, P. C., Sprenger, H.-G., Puszynska, A. M., Mann, J. L., Roessler, J. M., . . . Sabatini, D. M. (2021). Fumarate is a terminal electron acceptor in the mammalian electron transport chain. *Science, 374*(6572), 1227-1237. doi:doi:10.1126/science.abi7495

Storz, J. F., Scott, G. R., & Cheviron, Z. A. (2010). Phenotypic plasticity and genetic adaptation to high-altitude hypoxia in vertebrates. *The Journal of Experimental Biology, 213*(24), 4125-4136. doi:10.1242/jeb.048181

Tian, H., Zhang, B., Li, L., Wang, G., Li, H., & Zheng, J. (2020). Manipulation of Mitochondrial Plasticity Changes the Metabolic Competition Between "Foe" and "Friend" During Tumor Malignant Transformation. *Frontiers in Oncology, 10*. doi:10.3389/fonc.2020.01692

Vann, S. D., Aggleton, J. P., & Maguire, E. A. (2009). What does the retrosplenial cortex do? *Nature Reviews Neuroscience, 10*(11), 792-802. doi:10.1038/nrn2733

Wang, Z., Zhang, J., Ying, Z., & Heymsfield, S. B. (2012). Organ-Tissue Level Model of Resting Energy Expenditure Across Mammals: New Insights into Kleiber's Law. *ISRN Zoology, 2012*, 9. doi:10.5402/2012/673050

Watt, I. N., Montgomery, M. G., Runswick, M. J., Leslie, A. G. W., & Walker, J. E. (2010). Bioenergetic cost of making an adenosine triphosphate molecule in animal mitochondria. *Proceedings of the National Academy of Sciences, 107*(39), 16823-16827. doi:10.1073/pnas.1011099107

Yan, X., Zhang, J., Shi, J., Gong, Q., & Weng, X. (2010). Cerebral and functional adaptation with chronic hypoxia exposure: A multi-modal MRI study. *Brain research, 1348*, 21-29. doi:https://doi.org/10.1016/j.brainres.2010.06.024

Zhang, M., Cheng, Y., Zhai, Y., Cui, Y., Zhang, W., Sun, H., . . . Sun, H. (2022). Attenuated succinate accumulation relieves neuronal injury induced by hypoxia in neonatal mice. *Cell Death Discovery, 8*(1), 138. doi:10.1038/s41420-022-00940-7

Zungu, M., Young, M. E., Stanley, W. C., & Essop, M. F. (2008). Expression of mitochondrial regulatory genes parallels respiratory capacity and contractile function in a rat model of hypoxia-induced right ventricular hypertrophy. *Molecular and Cellular Biochemistry, 318*(1), 175-181. doi:10.1007/s11010-008-9867-5

Supplement

Table S1. Primers used for RT-qPCR

		Rats	Mice
Drp1	F:	5'-TCCAGAGAGGTAGATCCAGATG-3'	5'-AGAAGCAACCAGATGAACAAGA-3'
	R:	5'-AACCCTTCCCATCAATACATCC-3'	5'-AGTCAGCACAAACCAGTACTC-3'
DNM2	F:	5'-ATCACCAAGCTAGACCTGATG-3'	5'-AGAGAATGAGGATGGAGCACAAGAG-3'
	R:	5'-TTTCTGCCCTCGATGTCTTTC-3'	5'-TTTGGCATAAGGTCACGGATGGA-3'
MFN1	F:	5'-GATTGATAAGTTCTGCCTTGATGC-3'	5'-AGCAAGGATGTAACCACTACTAAACA-3'
	R:	5'-CCGCTCATTCACCTTATGGAA-3'	5'-CTAAAGAGAGAGAGCAGGAAAGCA-3'
MFN2	F:	5'-TGACTCCAGCCATGTCCAT-3'	5'-TAAAGGATGTAGCAGGAGGAA-3'
	R:	5'-CCATGTGTCGCTTATCCTTCT-3'	5'-TGTAGCAAGGCAGGGATGAG-3'
PGC1-α	F:	5'-ACCCACAGAGAACAGAAACAG-3'	5'-TGGGTGTGCGTGTGTGTATGT-3'
	R:	5'-GTTCAGAGGAAGAGATAAAGTTGT-3'	5'-GTCGCCCTTGTTCGTTCTGTTC-3'
TFAM	F:	5'-AGCTAAACACCCAGATGCAA-3'	5'-AGCAGGCACTACAGCGATACA-3'
	R:	5'-GTACACCTTCCACTCAGCTTT-3'	5'-AGCAGGCACTACAGCGATACA-3'
NRF1	F:	5'-GATGCTTCAGAACTGCCAAC-3'	5'-AGCCTCCATCTTCTCCCTTCC-3'
	R:	5'-GTCATTTCACCGCCCTGTA-3'	5'-AACACTTCTGTCACCTTCAGTTTGT-3'